Two-echelon multi-commodity multimodal vehicle routing problem considering user heterogeneity in city logistics

Wang, Shuai; Zhu, Xiaoning; Shang, Pan; Lin, Xiao; Yang, Liya; Tavasszy, Lóránt

DOI
10.1016/j.eswa.2024.124141

Publication date
2024

Document Version
Final published version

Published in
Expert Systems with Applications

Expert Systems With Applications 252 (2024) 124141

Contents lists available at ScienceDirect

Expert Systems With Applications

journal homepage: www.elsevier.com/locate/eswa

Two-echelon multi-commodity multimodal vehicle routing problem considering user heterogeneity in city logistics

Shuai Wang [a], Xiaoning Zhu [a], Pan Shang [a,*], Xiao Lin [b], Liya Yang [c,*], Lóránt Tavasszy [b]

[a] School of Traffic and Transportation, Beijing Jiaotong University, Beijing 100044, China
[b] Department of Transport and Planning, Delft University of Technology, Delft 2628CN, the Netherlands
[c] School of Public Administration, Renmin University of China, Beijing 100872, China

ARTICLE INFO

Keywords:
City logistics
Two-echelon vehicle routing problem
Multi-commodity
Multimodal transport
Adaptive large neighborhood search

ABSTRACT

The considerable increase in parcel deliveries has negatively impacted the accessibility and livability of cities. One solution strategy is to decouple short-distance from long-distance shipping so that last-mile transport can be performed with low-footprint vehicles. Such solutions are referred to in the literature as multi-echelon distribution systems. This study introduced a new variant of the two-echelon vehicle routing problem that considers multiple alternative transport modes as well as multiple commodities over a multi-period time horizon, where customers can obtain their commodities from any store. We referred to this problem as the two-echelon multi-commodity multimodal vehicle routing problem (MCM-2E-VRP). The objective of service providers is to minimize total generalized costs while satisfying customer requirements. We formulated this as a mathematical model based on a space–time network and introduced a random utility discrete choice model to capture variations in performance and preferences. We developed an adaptive large-neighborhood search (ALNS) algorithm to provide solutions for newly generated MCM-2E-VRP instances based on the Beijing Yizhuang transportation network. Extensive numerical experiments were conducted to verify the effectiveness of the proposed model and algorithm. A sensitivity analysis revealed some policy-relevant findings regarding the effects of store distribution and vehicle capacity.

1. Introduction

The rapid development of the express delivery industry has led to substantial increase in shipping activities in urban areas, contributing to traffic congestion and environmental problems. City logistics managers struggle to design cost-efficient and environmentally friendly last-mile delivery services. One solution strategy is to decouple short-distance from long-distance shipping so that last-mile transport can be performed with low-footprint vehicles. In the literature, such delivery configurations are known as multi-echelon distribution systems, particularly, two-tiered systems (Crainic, Ricciardi, & Storchi, 2009). The first echelon connects one or more facilities to multiple intermediate facilities in a larger urban area, and the second echelon (SE) connects the intermediate facilities to customers. The problem of vehicle routing in such systems is known as the two-echelon vehicle routing problem (2E-VRP) (Sluijk et al., 2023). The 2E-VRP aims to determine a set of minimal-cost routes for first-echelon and SE vehicles.

To reduce the challenges associated with freight transport while providing a cost-efficient and environmentally friendly distribution operation, transportation managers may consider the use of multiple city logistics elements such as buses, trams, and trucks to transport commodities. Although some researchers, such as Fontaine, Crainic, Jabali, and Rei (2021) and Vincent, Jodiawan, Schrotenboer, and Hou (2023), considered multiple transport modes to be available in the first echelon, the relevant literature is still limited, and the distribution of commodities in different transport modes is worthy of further discussion. Motivated by a realistic case for the collection and delivery of fresh agri-food products, the multi-commodity two-echelon distribution problem (MC2DP), another variant of the 2E-VRP, has been reported (Gu et al., 2022). The explicit consideration of multiple commodities is essential in city logistics, as it enables the joint optimization of transportation plans and the satisfaction of customer demands. Multiple commodities in a multi-period horizon can be considered as a component of future research (Gu et al., 2022). Therefore, in this study, we

* Corresponding authors.
E-mail addresses: 19114054@bjtu.edu.cn (S. Wang), xnzhu@bjtu.edu.cn (X. Zhu), shangpan@bjtu.edu.cn (P. Shang), yangliya@ruc.edu.cn (L. Yang), L.A.tavasszy@tudelft.nl (L. Tavasszy).

https://doi.org/10.1016/j.eswa.2024.124141
Received 12 December 2023; Received in revised form 16 April 2024; Accepted 29 April 2024
Available online 3 May 2024

proposed a new variant of the 2E-VRP, the two-echelon multi-commodity multimodal vehicle routing problem, considering user heterogeneity. The studied problem is a complex dynamic transportation system involving multiple transport modes to transport commodities in the first echelon and multiple commodities supplied from pickup locations, called stores. The service design determines the distribution path for logistics services, including the allocation to transportation modes.

The first feature of this study was the multiple transport modes that make use of multiple city logistics elements to transport commodities to satisfy customer requirements as much as possible. Since Perboli et al. (2011) coined the term 2E-VRP, several variants have been proposed (Cuda, Guastaroba, & Speranza, 2015; Sluijk, Florio, Kinable, Dellaert, & Van Woensel, 2023). Most studies focused on a single transport mode in each echelon. Fontaine et al. (2021) were the first to investigate two-tier multiple city logistics elements, including line-based and other transport modes. Line-based transport modes usually include regular and light rail tramways, whereas other transport modes include various trucks and barges. Bayliss, Bektaş, Tjon-Soei-Len, and Rohner (2023) introduced a multimodal variable-echelon last-mile delivery system. In contrast to Fontaine et al. (2021), this study used multiple transport modes to transport commodities by considering the heterogeneity of users. The second important feature of this study was the presence of multiple commodities. Multiple commodities were collected from stores and delivered to communities via satellites or hubs for consolidation. Only two recent studies considered multiple commodities in the context of the 2E-VRP. Gu et al. (2022) were the first to make route decisions considering multiple commodities in two-echelon distribution problems and introduced the multi-commodity two-echelon distribution problem for the 2E-VRP. Jia, Deng, Zhao, and Chen (2023) also studied route optimization with multiple commodity requests, where each customer could obtain two commodities from two depots. Although the recent literature has discussed the benefits of multiple transport modes and commodities, their integration into the 2E-VRP has not yet been considered. In this study, we combined these two features into one model.

The contributions of this study are as follows. First, we defined a new two-echelon vehicle routing problem that integrates multiple transport modes, considering the heterogeneity of users and multiple commodities in a multi-period horizon, known as the MCM-2E-VRP. Second, we formulated a mathematical model for the MCM-2E-VRP based on a space–time network and introduced a random utility discrete choice model to capture user heterogeneity. An adaptive large neighborhood search (ALNS) algorithm was developed to solve the MCM-2E-VRP. Some modifications were made to adapt the characteristics of the MCM-2E-VRP. Finally, we performed extensive numerical experiments to demonstrate the efficiency of the proposed model and algorithm and analyzed the impacts of store distribution and vehicle capacity.

The remainder of the paper is organized as follows. Section 2 provides a review of the related literature. Section 3 describes the problem statement and presents the mathematical formulation of the model. The solution algorithm is outlined in Section 4. Section 5 presents and discusses the results of the numerical experiments, including the sensitivity analysis. Finally, section 6 concludes the paper and provides suggestions for future research.

2. Literature review

In this section, we review research related to the MCM-2E-VRP, including the baseline 2E-VRP model, its extension toward multimodality, and its multi-commodity variant (MC-2E-VRP).

The study of the 2E-VRP was initiated by Crainic et al. (2009), who formalized the two-echelon, synchronized, scheduled, multi-depot, multiple-tour, heterogeneous vehicle-routing problem with time windows. Perboli, Tadei, and Vigo (2011) introduced a mathematical model and two heuristics for the 2E-VRP. Most existing literature on the 2E-VRP utilizes heuristic methods to solve the 2E-VRP, including local neighborhood search (Belgin, Karaoglan, & Altiparmak, 2018), adaptive large neighborhood search (Hemmelmayr, Cordeau, & Crainic, 2012; Grangier, Gendreau, Lehuédé, & Rousseau, 2016), genetic algorithms (Wang, Lan, & Zhao, 2017; Zhou, Baldacci, Vigo, & Wang, 2018), and path relinking (Anderluh, Hemmelmayr, & Nolz, 2017). Exact methods for the 2E-VRP have also been investigated. Baldacci, Mingozzi, Roberti, and Calvo (2013) proposed a customized exact method with a bounding procedure to decompose the two-echelon capacity vehicle routing problem (2E-CVRP). Santos, Mateus, and da Cunha (2015) and Marques, Sadykov, Deschamps, and Dupas (2020) proposed branch-and-cut-and-price algorithms for the 2E-CVRP. For a broader overview of research on the 2E-VRP, refer to the literature reviews by (Cuda et al., 2015; Sluijk et al., 2023). Over the years, many variants of the 2E-VRP have emerged in the literature, based on various problems encountered in real-world vehicle routing applications, such as time windows (Vincent et al., 2023; Zhou, Zhang, Ji, & Li, 2024), drones (Zhou, Qin, Cheng, & Rousseau, 2023), simultaneous pickup and delivery (Yıldız, Karaoğlan, & Altiparmak, 2023), and collaborative delivery (Kim, Jeong, & Lee, 2023).

Research on multimodal city logistics has increased over the past decade. However, most studies have focused on single-echelon multimodal city logistics. Perboli, Rosano, Saint-Guillain, and Rizzo (2018) proposed a simulation–optimization framework and applied it to an online parcel delivery problem to evaluate the impact of multimodal delivery options on e-commerce demand in the urban context of Turin. Liu, Lyu, Liu, and Cao (2021) investigated a city-wide multimodal transportation recommendation system (MTRS). Najmi, Rashidi, and Waller (2023) proposed a multi-class, multimodal, and multi-provider market equilibrium (MCMPE) model to evaluate the operation of transport systems. Multimodal transport includes private vehicles, walking, public transport, ride-sourcing, ridesharing-as-driver, ridesharing-as-rider, and crowd-shipping. Customer choices between these shipping options can be described using random utility discrete choice models (Wicaksono, Lin, & Tavasszy, 2022; Tapia, Kourounioti, Thoen, de Bok, & Tavasszy, 2023; Cebeci, Tapia, Kroesen, de Bok, & Tavasszy, 2023). Very few studies have discussed two-echelon multimodal city logistics. Fontaine et al. (2021) addressed the tactical planning problem for a two-tier multimodal city logistics (2TM-CL) system that integrated inbound and outbound demands and different transportation modes. Vincent et al. (2023) introduced the concept of crowd-shipping, which utilizes the extra capacity of on-road vehicles to deliver small demands, and proposed a two-echelon vehicle routing problem with time windows, intermediate facilities, and occasional drivers (2E-VRPTW-IF-OD). Customers can receive goods delivered by either city freighters or occasional drivers to their homes or perform self-pickup at selected parcel lockers. Bayliss et al. (2023) proposed a last-mile logistics delivery system that utilized multiple localized storage depots and multimodal delivery options.

The MC-2E-VRP was developed by Sluijk et al. (2023) as an extension of the traditional 2E-VRP. Studies on the MC-2E-VRP generally assume that each commodity is provided by a unique depot, as in Crainic, Errico, Rei, and Ricciardi (2016), Kancharla and Ramadurai (2019), and Dellaert, Van Woensel, Crainic, and Saridarq (2021). Boccia, Crainic, Sforza, and Sterle (2018) studied a multi-commodity location-routing problem (LRP) in city logistics systems, known as the flow-intercepting facility LRP (FIFLOR). Here, each commodity has only one origin–destination path. We are aware of only two studies that have explicitly considered multiple commodities. Gu et al. (2022) presented an MC2DP for a many-to-many setting in which each commodity was collected from any origin offering it and delivered to any destination requiring it. Jia et al. (2023) introduced a multi-commodity two-echelon vehicle routing problem with satellite synchronization. In this problem, each customer obtained two commodities from two depots.

Table 1 summarizes the related literature regarding the studied problems, including the structure of the logistics network, problem features, models, algorithms, and case studies. As the literature survey

Table 1
Summary of the related literature on the problem features of the MCM-2E-VRP.

Reference	Problem	Structure of logistics network	Multi-modal	Multi-commodity	Model	Solution algorithm	Case study
Liu et al. (2021)	Multi-modal transportation	VRP	√		MTRS	A post-processing algorithm	Baidu Maps, China
Najmi et al. (2023)	Transport system planning	VRP	√		MCMPE	Karush–Kuhn–Tucker optimality conditions	Sydney, Australia
Fontaine et al. (2021)	2TM-CL	2E-VRP	√		MILP	Benders decomposition algorithm	Synthetical data
Vincent et al. (2023)	2E-VRPTW-IF-OD	2E-VRP	√		MILP	Hybrid ALNS algorithm	Synthetical data
Bayliss et al. (2023)	Last-mile delivery	Variable-echelonVRP	√		MILP	A scalable two-phase heuristic algorithm	London, England
Boccia et al. (2018)	FIFLOR	LRP		√	ILP	Branch-and-cut algorithm	Synthetical data
Gu et al. (2022)	MC2DP	2E-VRP		√	MIP	Two sequential approaches	Isere, French
Jia et al. (2023)	MC-2E-VRPSS	2E-VRP		√	MIP	ALNS algorithm	Synthetical data
This paper	MCM-2E-VRP	2E-VRP	√	√	MILP	ALNS algorithm	Beijing, China

MTRS: Multimodal transportation recommendation system; MCMPE: Multi-class multimodal multi-provider market equilibrium; MILP: mixed-integer linear program; ILP: integer integer program; MIP: mixed-integer program.

shows, research investigating the features of multimodality or multi-commodity remains limited in the 2E-VRP literature, and the integration of the two features in the 2E-VRP is absent. This study aimed to fill this gap by introducing a new two-echelon vehicle-routing problem that integrates two features: multimodality and multi-commodity. Unlike previous studies that selected the transport mode based on the total generalized cost, such as Fontaine et al. (2021) and Vincent et al. (2023), this study utilized multiple transport modes to transport commodities by considering the heterogeneity of users. Meanwhile, we used a many-to-one logistics setting in which multiple commodities can be collected from any store and customers can obtain their commodities in a multi-period horizon. Then, we constructed a new model that addressed the following dimensions: (1) assigning a distribution route for each commodity in a many-to-one logistics setting, and (2) selecting a transport mode to transport commodities considering the heterogeneity of users in a multimodal setting. The consideration of these two features increases the complexity of solving the model; thus, the ALNS algorithm was used to solve the model. Extensive numerical experiments were conducted to verify the efficiency of the proposed method.

3. Problem statement and model formulation

3.1. Problem statement

We present the MCM-2E-VRP below as an illustrative case, as shown in Fig. 1. The MCM-2E-VRP consists of two echelons. In the first echelon, commodities can be transported using different modes of transport. In the example, the city logistics service includes three transport modes: rigid truck transport, trailer truck transport, and public transport. SE vehicles are used for pickup and delivery operations in the SE. Each store contains a variety of commodities, and the customer requirements in each community represent a single type of commodity. Satellites facilitate the transshipment of commodities between vehicles. We assume that shipping requests are served by a logistics company or a third-party platform, referred to as the supplier. The supplier provides logistics network information, including storage information, *trans*-shipment information, distances between satellites, and information on different transport modes. All travel times for each link, service times, and transfer times in the logistics network are known in advance. In addition, the supplier sets capacity limits for different transport modes. User heterogeneity is an important motivation for transport mode choice. The supplier aims to minimize total delivery costs while meeting customer requirements.

Customers can select a transport mode that suits their requirements for delivering commodities based on the cost, time, and frequency of all transport modes. However, once suppliers fully outsource shipping functions, they realize the risk of losing control and visibility over freight movements. We assume that customers will be willing to transfer mode selection authority to the service provider under certain conditions (Khakdaman, Rezaei, & Tavasszy, 2020) and that the supplier is trusted to choose a transport mode according to the preferences of customers. The route-choice behavior considered in this study is determined by the supplier. For instance, if the customer pursues minimum transport cost and pays no attention to time, the supplier will prioritize selecting public transport to deliver the commodities. We applied a mixed logit model to describe the variations in user preferences.

We assume that multiple commodities in each store must be delivered to different communities. In the SE, each vehicle can transport multiple commodities within the city if its capacity is not exceeded. Service design is established for short periods and is repeatedly carried out throughout the planning horizon. We assume that the service design cannot be modified during shipping, and that public transport is used as a part of freight services without affecting the passenger service level. Moreover, we assume that public transport has a finite capacity for freight shipments, in addition to the available spaces for passengers. Thus, it is possible that the capacity of public transport is insufficient to satisfy freight shipments. Suppliers may readjust the shipping service to achieve the demand–supply balancing in the system. A first-in-first-out

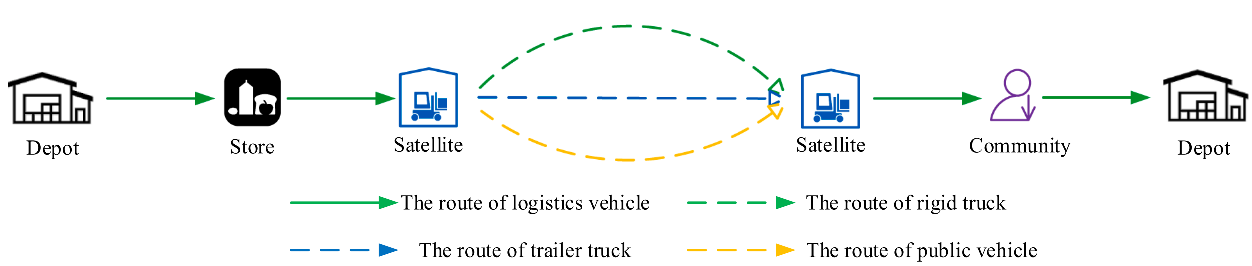

Fig. 1. Illustration of the MCM-2E-VRP.

policy can be applied to readjust the commodity allocations.

An example of a stylized physical network for the MCM-2E-VRP is shown in Fig. 2. The network is composed of five types of nodes and two types of links. The number in the link represents the distance between two nodes. SE vehicles with a capacity of 10 pieces collect commodities from four stores and deliver them to two communities in the SE, whereas different transport modes can be adopted for shipping services in the first echelon. Here, the rigid truck capacity is set to 10, and the capacities of the trailer trucks and public vehicles are assumed to be sufficient. We assume that the fixed cost of each rigid truck, trailer truck, and public vehicle is two units, three units, and zero per vehicle, respectively, and this unit represents a cost unit, such as the euro. The average velocities of rigid trucks, trailer trucks, and public vehicles are 2 distances/mins, 1.2 distances/mins, and 1 distance/min, respectively, in the first echelon. In the SE, the capacity of the SE vehicles is set to 10, the fixed cost of each SE vehicle is one unit, and the average velocity of the SE vehicles is assumed to 1 distance/min. We assume that the travel cost of different trucks is the ratio of the corresponding travel time, and the ratios of SE vehicles, rigid trucks, trailer trucks, and public vehicles are 1, 0.6, 0.3, and 0.2, respectively, in this network. The transfer time at the satellite facilities is set to 5 min. The planning horizon consists of three periods, each set at 90 min. The commodities are randomly generated during each period.

In the constructed network, the supplier designs three routes for different transport modes and provides relevant attributes of the transport modes, including cost, time, and frequency. The supplier can choose a suitable transport mode to deliver commodities to customers based on the attributes of the transport mode. Furthermore, the supplier can readjust customer requirements to satisfy the capacities of different transport modes. Finally, the demand–supply balancing for the service system is achieved, as illustrated in Fig. 3.

3.2. Space–time network construction

For convenience in constructing the mathematical model, the MCM-2E-VRP can be divided into three stages: pickup, transport, and delivery. The studied problem can be defined on a graph $G = (N, A)$, where $N = N^P \cup N^T \cup N^D$ and $A = A^P \cup A^T \cup A^D$ based on different stages. Moreover, T is a planning horizon, indexed by $t, t' \in T$. In the pickup and delivery stages, the SE vehicles K^P/K^D with capacity Q^{PD} are dispatched to visit a set of pickup and delivery sites. In the transport stage, the transport trucks K^T, including rigid trucks, trailer trucks, and public vehicles, are used to transport commodities. The three transport modes in the transport stage are indexed by $w \in W$. For different transport modes, the speed, unit travel cost, and fixed cost of truck k at link (i,j) are defined as v_{k_w}, $c^w_{i,j}$, and fc^w_k, respectively. For each link $(i,j) \in A$, the travel distances $d_{i,j}$ are defined. The notations used are listed in Table 2.

Although the space–time network graph is more complex than the physical network graph, the number of parameters can be reduced effectively because the time factor is incorporated into the space–time network. The space–time network is composed of vertice-arcs, where vertex (i,t) replaces node i and arc (i,j,t,t') substitutes link (i,j). Constraints related to time windows, such as the time window $[e_{\tau l}, l_{\tau l}]$ of each store l, the latest delivery time $l_{\tau u}$ for community u at each period τ, are embedded into the space–time network. The total commodity volumes are considered as known inputs, but the commodities for each transport mode must be determined by the customer's route-choice behavior. The commodities $q_{\tau l} = [q^0_{\tau l}, q^1_{\tau l}, \cdots, q^u_{\tau l}]$ randomly generated are picked up at the store l and delivered to the community u at each period τ. Each store and community has a fixed service time of st, and each satellite has a specific transfer time of wt. The timetables of each transport mode $w \in W$ are also a known input.

The constructed space–time network of the illustrated instance is shown in Fig. 4. In the pickup stage, SE vehicles run from the origin depot to the satellite facilities and pick up commodities from several stores along their journey. The arc of the SE vehicles (i,j,t,t') represents the vehicles starting from node i at time t to node j at time t', where $(t' - t)$ is the travel time of link (i,j) plus the service time at node j. Note that the service time is set to zero in the illustrated instance. In the transport and delivery stages, if the supplier chooses different transport modes, different transport paths are generated. When commodities are transferred to satellite facilities, the transfer arc (i,i,t,t') is created to connect with different trucks.

3.3. Mathematical model for the MCM-2E-VRP

To optimize vehicle routing considering user heterogeneity, the MCM-2E-VRP was formulated as a mixed-integer linear programming model, and customer route-choice behavior was modeled using the mixed logit model.

3.3.1. Model formulation

The objective of the proposed problem is to minimize the total generalized costs while satisfying customer requirements, which consist of the pickup cost (Z_p), delivery cost (Z_d), and transport cost (Z_w), including the cost of rigid trucks (Z_1), trailer trucks (Z_2), and public vehicles (Z_3), as shown in equations (1)–(4). In the objective function, the fixed cost fc^3_k of a public vehicle k, such as a bus or subway, is not considered.

$$\min Z = Z_p + Z_d + Z_w \tag{1}$$

$$Z_p = \sum_{\tau \in T}\sum_{k \in K^P}\sum_{(i,j,t,t') \in A^P} c_{i,j,t,t'} \bullet x^{\tau p}_{i,j,t,t',k} + \sum_{\tau \in T}\sum_{k \in K^P} fc_k \bullet y^{\tau p}_k \tag{2}$$

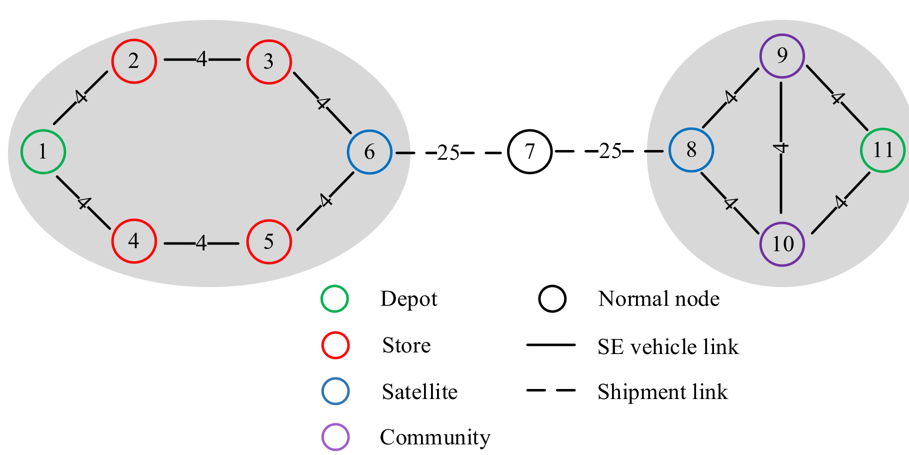

Fig. 2. Physical network of the MCM-2E-VRP.

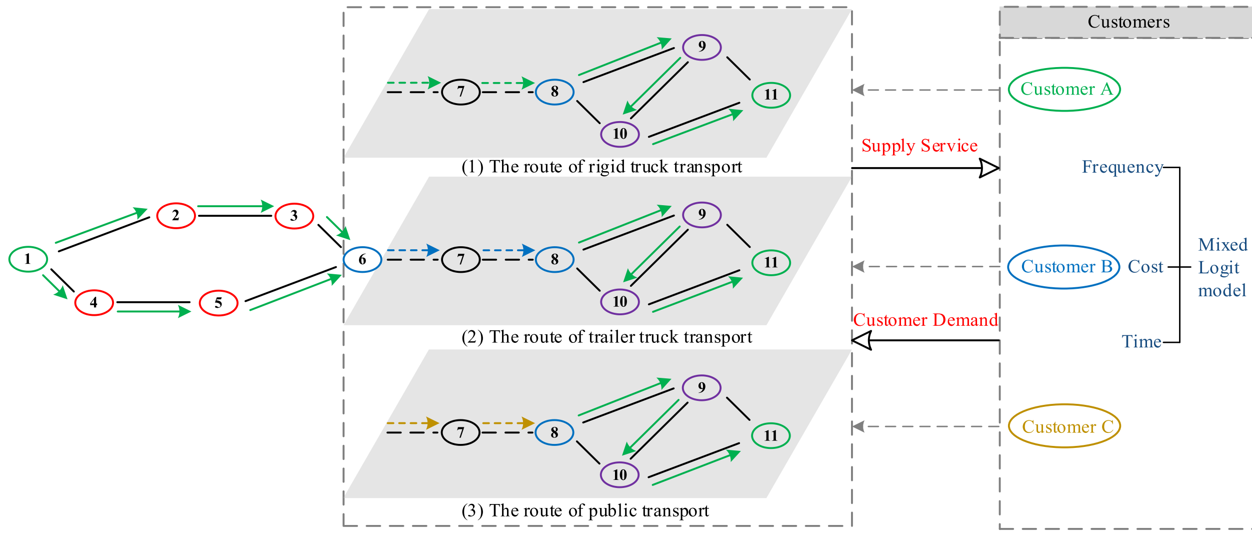

Fig. 3. Demand–supply balancing for the service system.

$$Z_d = \sum_{\tau\in T}\sum_{k\in K^D}\sum_{(i,j,t,t')\in A^D} c_{i,j,t,t'} \bullet x^{\tau d}_{i,j,t,t',k} + \sum_{\tau\in T}\sum_{k\in K^D} fc_k \bullet y^{\tau d}_k \tag{3}$$

$$Z_w = \sum_{\tau\in T}\sum_{k_w\in K}\sum_{w\in W}\sum_{(i,j,t,t')\in A^T} c^w_{i,j,t,t'} \bullet x^{\tau t}_{i,j,t,t'k_w} + \sum_{\tau\in T}\sum_{k_w\in K}\sum_{w\in W} fc^w_k \bullet y^{\tau t}_{k_w} \tag{4}$$

These constraints include the following four categories: constraints at the pickup stage, delivery stage, and transport stage, and synchronization constraints.

Constraints in the pickup stage

Constraints (5)–(7) represent the flow-balance constraints at the pickup stage. Constraints (5) and (6) define that each vehicle k begins at origin $o, o \in N^P$ and ends at the satellite facility $to, to \in N^T$, respectively. Constraint (7) guarantees that the input flow is consistent with the output flow at the other intermediate nodes. Constraint (8) ensures that all commodities are selected. Constraint (9) represents the capacity of SE vehicles for commodity pickup. Constraint (10) states that SE vehicle k can serve at any store no more than once.

$$\sum_{(o,j,t,t')\in\delta^-(o,t)} x^{\tau p}_{o,j,t,t',k} = 1 \forall \tau \in T, k \in K^P, (o,j,t,t') \in A^P \tag{5}$$

$$\sum_{(j,to,t,t')\in\delta^+(to,t')} x^{\tau p}_{j,to,t,t',k} = 1 \forall \tau \in T, k \in K^P, (j,to,t,t') \in A^P \tag{6}$$

$$\sum_{(i,j,t,t')\in\delta^+(j,t')} x^{\tau p}_{i,j,t,t',k} - \sum_{(j,j',t',t'')\in\delta^-(j,t')} x^{\tau p}_{j,j',t',t'',k} = 0 \forall \tau \in T, k \in K^P, j \in N^P and j \neq o, to \tag{7}$$

$$\sum_{k\in K^P}\sum_{(j,j',t',t'')\in\delta^-(j,t')} f^{\tau u}_{j,j',t',t'',k} - \sum_{k\in K^P}\sum_{(i,j,t,t')\in\delta^+(j,t')} f^{\tau u}_{i,j,t,t',k} = q^u_{\tau j} \forall \tau \in T, j \in N^L, u \in N^U \tag{8}$$

$$0 \le \sum_{u\in N^U} f^{\tau u}_{i,j,t,t',k} \le Q^{PD} \bullet x^{\tau p}_{i,j,t,t',k} \forall \tau \in T, k \in K^P, (i,j,t,t') \in A^P \tag{9}$$

$$\sum_{(i,j,t,t')\in\delta^+(j,t')} x^{\tau p}_{i,j,t,t',k} \le y^{\tau p}_k \forall \tau \in T, k \in K^P, j \in N^L \tag{10}$$

Constraints in the transport stage

Constraints (11)–(13) represent the flow-balance constraints at the transport stage. Constraints (11) and (12) guarantee that each truck k_w begins at one satellite facility $to, to \in N^T$ and ends at another satellite facility $td, td \in N^T$, respectively. Constraint (13) ensures that the input flow is the same as the output flow at the other intermediate nodes. Constraint (14) indicates that the commodities are consistent at the transport nodes. Constraint (15) specifies the capacity of each truck. Constraint (16) guarantees that a transport node is visited no more than once by vehicle k_w.

$$\sum_{(to,j,t,t')\in\delta^-(to,t)} x^{\tau t}_{to,j,t,t',k_w} = 1 \forall \tau \in T, k_w \in K^T, w \in W, (to,j,t,t') \in A^T \tag{11}$$

$$\sum_{(j,td,t,t')\in\delta^+(td,t')} x^{\tau t}_{j,td,t,t',k_w} = 1 \forall \tau \in T, k_w \in K^T, w \in W, (j,td,t,t') \in A^T \tag{12}$$

$$\sum_{(i,j,t,t')\in\delta^+(j,t')} x^{\tau t}_{i,j,t,t',k_w} - \sum_{(j,j',t',t'')\in\delta^-(j,t')} x^{\tau t}_{j,j',t',t'',k_w} = 0 \forall \tau \in T, k_w \in K^T, w \in W, j \in N^T and j \neq to, td \tag{13}$$

$$\sum_{(i,j,t,t')\in\delta^+(j,t')} f^{\tau u}_{i,j,t,t',k_w} - \sum_{(j,j',t',t'')\in\delta^-(j,t')} f^{\tau u}_{j,j',t',t'',k_w} = 0 \forall \tau \in T, k_w \in K^T, j \in N^T, u \in N^U, w \in W \tag{14}$$

$$0 \le \sum_{(i,j,t,t')\in\delta^+(j,t')} f^{\tau u}_{i,j,t,t',k_w} \le Q^T \bullet x^{\tau t}_{i,j,t,t',k_w} \forall \tau \in T, k_w \in K^T, (i,j,t,t') \in A^T, w \in W \tag{15}$$

$$\sum_{(i,j,t,t')\in\delta^+(j,t')} x^{\tau t}_{i,j,t,t',k_w} \le y^{\tau t}_{k_w} \forall \tau \in T, k_w \in K^T, w \in W, j \in N^T \tag{16}$$

Constraints in the delivery stage

Constraints (17)–(19) represent the flow-balance constraints at the delivery stage. Constraints (17) and (18) indicate that each SE vehicle k starts at satellite facility $td, td \in N^T$ and ends at destination $d, d \in N^D$, respectively. Constraint (19) ensures that the input flow is consistent with the output flow at the other intermediate nodes. Constraint (20) guarantees that all delivery requests are satisfied. Constraint (21) guarantees the capacity of the SE vehicle for commodity delivery. Constraint (22) indicates that SE vehicle k can serve a community no more than once.

$$\sum_{(td,j,t,t')\in\delta^-(td,t)} x^{\tau d}_{td,j,t,t',k} = 1 \forall \tau \in T, k \in K^D, (td,j,t,t') \in A^D \tag{17}$$

$$\sum_{(j,d,t,t')\in\delta^+(d,t')} x^{\tau d}_{j,d,t,t',k} = 1 \forall \tau \in T, k \in K^D, (j,d,t,t') \in A^D \tag{18}$$

Table 2
Notations used for formulating the MCM-2E-VRP.

Notation	Definition
Set and Parameters	
N	Set of nodes in the transportation network, $N = N^P \cup N^T \cup N^D$, where N^P is the set of nodes at the pickup stage, N^T is the set of nodes at the transport stage, and N^D is the set of nodes at the delivery stage
N^L	Set of stores,$N^L \in N^P$
N^U	Set of communities,$N^U \in N^D$
A	Set of links in the transportation network, $A = A^P \cup A^T \cup A^D$, where A^P is the set of links at the pickup stage, A^T is the set of links at the transport stage, and A^D is the set of links at the delivery stage
$\delta^+(i,t)$	Set of links in A whose tail is node i at time t
$\delta^-(i,t)$	Set of links in A whose head is node i at time t
T	Set of time intervals
W	Set of transport modes
K	Set of vehicles, $K = K^P \cup K^D \cup K^T$, where K^P is the set of SE vehicles at the pickup stage, K^D is the set of SE vehicles at the delivery stage, and K^T is the set of the transport trucks, including rigid trucks, trailer trucks, and public vehicles
Q^{PD}	Capacity of SE vehicles,$K^P \cup K^D$
Q^T_w	Capacity of transport trucks,$k_w \in K^T$
i,j,j'	Index of nodes,$i,j,j' \in N$
(i,j)	Index of links,$(i,j) \in A$
d_{ij}	Index of distance at link (i,j)
t,t'	Index of time intervals,$t,t' \in T$
τ	Index of time periods,$\tau \in T$
w	Index of transport modes,$w \in \{1,2,3\}$
k	Index of vehicles,$k \in K^P \cup K^D$
k_w	Index of trucks,$k_w \in K^T$
v_{k_w}	Index of speed of truck k_w
$q_{\tau l}$	Index of commodity of store l at period τ, $q_{\tau l} = [q^0_{\tau l}, q^1_{\tau l}, \cdots, q^u_{\tau l}]$
$q^u_{\tau l}$	Index of commodity of store l to community u at period τ
c_{ij}	Unit of travel cost of SE vehicle at link (i,j)
c^w_{ij}	Unit travel cost of different terms, $w \in \{1,2,3\}$. c^1_{ij} is the travel cost of the rigid truck at link (i,j), c^2_{ij} is the travel cost of the trailer truck at link (i,j), c^3_{ij} is the travel cost of the public vehicle at link (i,j)
fc_k	Unit fixed cost of SE vehicle k, $k \in K$
fc^w_k	Unit fixed cost of different terms, $w \in \{1,2,3\}$. fc^1_k is the fixed cost of rigid truck k, fc^2_k is the fixed cost of trailer truck k, and fc^3_k is the fixed cost of public vehicle k
(i,t), (j,t')	Index of space–time vertices
(i,j,t,t')	Index of space–time arcs
$[e_{\tau l}, l_{\tau l}]$	Time window of store l at period τ, where $e_{\tau l}$ is the earliest service time, and $l_{\tau l}$ is the latest service time
$l_{\tau u}$	Latest delivery time of community u at period τ
st	Service time at store and community
wt	Transfer time at the satellite
M	Sufficiently large positive integer
Decision variables	
$x^{\tau p}_{i,j,t,t',k}$	$= 1$ if SE vehicle k traverses arc (i,j,t,t') at period τ at the pickup stage, $(i,j,t,t') \in A^P$; $= 0$ otherwise
$x^{\tau t}_{i,j,t,t',k_w}$	$= 1$ if truck k_w traverses arc (i,j,t,t') at period τ by transport mode $w \in \{1,2,3\}$ at the transport stage, $(i,j,t,t') \in A^T$; $= 0$ otherwise
$x^{\tau d}_{i,j,t,t',k}$	$= 1$ if SE vehicle k traverses arc (i,j,t,t') at period τ at the delivery stage, $(i,j,t,t') \in A^D$; $= 0$ otherwise
$y^{\tau p}_k$	$= 1$ if SE vehicle k performs pickup operator at period τ at the pickup stage, $k \in K^P$; $= 0$ otherwise
$y^{\tau t}_{k_w}$	$= 1$ if truck k_w is used at period τ in the transport stage, $k_w \in K^T$; $= 0$ otherwise
$y^{\tau d}_k$	$= 1$ if SE vehicle k is used at period τ in the delivery stage, $k \in K^D$; $= 0$ otherwise
$f^{\tau u}_{i,j,t,t',k}$	Total load to unloading node u that is carried along arc (i,j,t,t') by vehicle k at period τ
$f^{\tau u}_{i,j,t,t',k_w}$	Total load to unloading node u that is carried along arc (i,j,t,t') by truck k_w at period τ

$$\sum_{(i,j,t,t')\in\delta^+(j,t')} x^{\tau d}_{i,j,t,t',k} - \sum_{(j,j',t',t'')\in\delta^-(j,t')} x^{\tau d}_{j,j',t',t'',k} = 0 \forall \tau \in T, k \in K^D, j \in N^D and j \neq td, d \tag{19}$$

$$\sum_{k\in K^D}\sum_{(u,j,t',t'')\in\delta^-(u,t')} f^{\tau u}_{u,j,t',t'',k} - \sum_{k\in K^D}\sum_{(i,u,t,t')\in\delta^+(u,t')} f^{\tau u}_{i,u,t,t',k} = \sum_{i\in N^L} q^u_{\tau i} \forall \tau \in T, u \in N^U \tag{20}$$

$$0 \leq \sum_{u\in N^U} f^{\tau u}_{i,j,t,t',k} \leq Q^{PD} \bullet x^{\tau d}_{i,j,t,t',k} \forall \tau \in T, k \in K^D, (i,j,t,t') \in A^D \tag{21}$$

$$\sum_{(i,j,t,t')\in\delta^+(j,t')} x^{\tau d}_{i,j,t,t',k} \leq y^{\tau d}_k \forall \tau \in T, j \in N^U, k \in K^D \tag{22}$$

Synchronization Constraints

Constraint (23) represents the consistency of commodity flows between the pickup and transport stages, in which $t' + wt \leq t''$, and the arrival time of SE vehicles is earlier than the departure time of transport trucks at a satellite facility. Constraint (24) states that all commodities should be transferred from transport trucks to SE vehicles, in which $t' + wt \leq t''$, and the arrival time of transport trucks is earlier than the departure time of SE vehicles. Because the arrival times of commodities in different transport modes in the transport stage are different, commodities in each transport mode are distributed by different groups of SE vehicles.

$$\sum_{k\in K^P}\sum_{(i,to,t,t')\in\delta^+(to,t')} f^{\tau u}_{i,to,t,t',k} - \sum_{w\in W}\sum_{k_w\in K^T}\sum_{(to,j,t'',t''')\in\delta^-(to,t'')} f^{\tau u}_{to,j,t'',t''',k_w} = 0 \forall \tau \in T, i \in N^P, j \in N^T, u \in N^U \tag{23}$$

$$\sum_{w\in W}\sum_{k_w\in K^T}\sum_{(i,td,t,t')\in\delta^+(td,t')} f^{\tau u}_{i,td,t,t',k_w} - \sum_{k\in K^D}\sum_{(td,j,t'',t''')\in\delta^-(td,t'')} f^{\tau u}_{td,j,t'',t''',k} = 0 \forall \tau \in T, i \in N^T, j \in N^D, u \in N^U \tag{24}$$

3.3.2. Route-choice behavior

The number of commodities can be obtained by selecting different transport modes based on their attributes. For each customer, there are three transport modes $w \in W = [1,2,3]$ of rigid trucks, trailer trucks, and public vehicles to select. In this study, a mixed logit model was adopted to handle customers' route-choice behavior. Mixed logit eliminates the three limitations of the standard logit by allowing random taste variation, unrestricted substitution patterns, and time-dependent correlations of unobserved factors (Train, 2009). The utility function is given by equation (25) and includes the cost, time, and frequency of each transport mode.

$$U_{w,\tau,u} = \beta^C_{w,\tau,u} \bullet X^C_{w,\tau,u} + \beta^T_{w,\tau,u} \bullet X^T_{w,\tau,u} + \beta^F_{w,\tau,u} \bullet X^F_{w,\tau,u} + \varepsilon_{w,\tau,u} \forall w \in W, \tau \in T, u \in N^U \tag{25}$$

The value $X^C_{w,\tau,u}$ denotes the total cost to deliver to community u by adopting transport mode w at period τ in the transport stage. The value $X^T_{w,\tau,u}$ represents the total time to deliver to community u using transport mode w at period τ in the transport stage. The value $X^F_{w,\tau,u}$ denotes the frequency of transport mode w to deliver to community u at period τ. The error term $\varepsilon_{w,\tau,\mu}$ is a random term that is iid of the extreme value type I.

The parameters in the mixed logit model were randomly distributed and each parameter was allowed to vary across observations and follow a predefined distribution form. For parameters with the same sign for all customers, a log-normal distribution was adopted in this study. For instance, the cost parameter $\beta^C_{w,\tau,u}$ that is negative follows a lognormal distribution with parameters u_c and σ^2_c. The equation of the cost parameter $\beta^C_{w,\tau,u}$ is expressed as follows, in which Z is a standard normal variable:

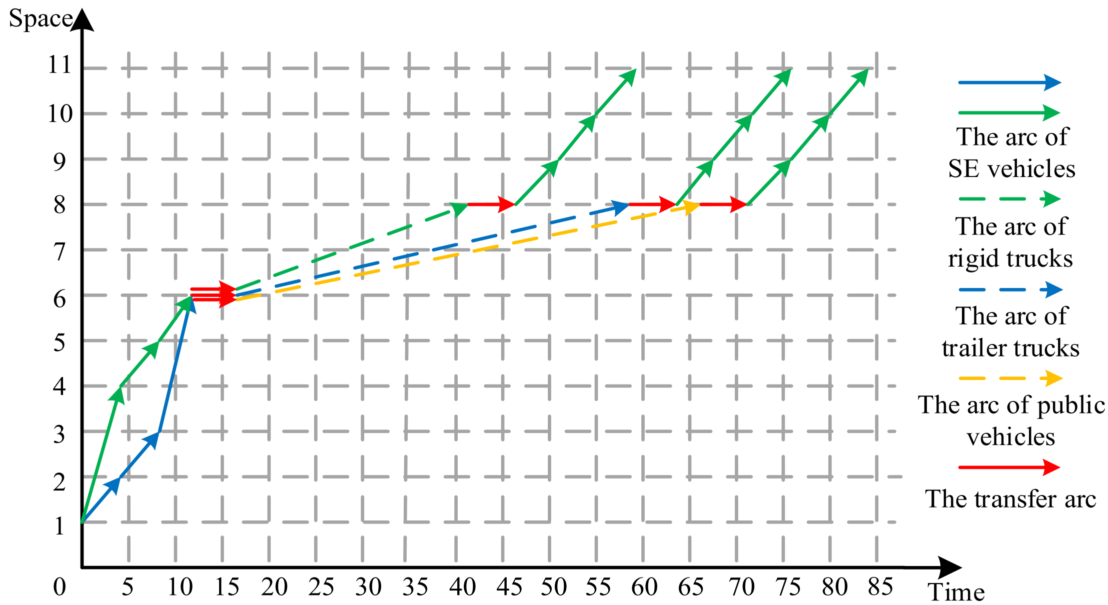

Fig. 4. Space–time network of the illustrated instance.

$$\beta^C_{w,\tau,u} = -e^{u_c+\sigma_c Z} \tag{26}$$

Subsequently, the mean $\overline{\beta^C_{w,\tau,u}}$ and variance $\sigma^2_{\beta^C_{w,\tau,u}}$ of the cost parameter $\beta^C_{w,\tau,u}$ can be obtained from equations (27) and (28). In this study, a maximum likelihood estimation with 10,000 draws in $N(0,1)$ was used to determine the parameter values.

$$\overline{\beta^C_{w,\tau,u}} = -e^{u_c+\sigma_c^2/2} \tag{27}$$

$$\sigma^2_{\beta^C_{w,\tau,u}} = \left(e^{\sigma_c^2}-1\right)e^{2u_c+\sigma_c^2} \tag{28}$$

Based on the utility function, we can obtain the probability, as shown in equation (29). The supplier can choose the transport mode w to deliver to community u at period τ for customers, and the commodities $f^{\tau u}_{i,j,t,t',k_w}$ for selecting transport mode w can be obtained using equation (30). Finally, returning the commodities $f^{\tau u}_{i,j,t,t',k_w}$ of transport mode w to construct the proposed optimization model, the minimum total generalized costs can be obtained.

$$P_{w,\tau,u} = e^{U_{w,\tau,u}} / \sum_{w\in W} e^{U_{w,\tau,\mu}} \tag{29}$$

$$f^{\tau u}_{i,j,t,t',k_w} = f^{\tau u}_{i,j,t,t',k} \times P_{w,\tau,\mu} \tag{30}$$

Because public vehicles give priority to passengers, the commodities $f^{\tau u}_{i,j,t,t',k_3}$ generated based on customers' route choice do not always match the capacity Q^T_3 of public vehicles for freight service, that is, $f^{\tau u}_{i,j,t,t',k_3} > Q^T_3$. Therefore, the capacity of public vehicles for freight services may be insufficient, causing customers to adopt other transport modes to satisfy their requirements. At this point, we adopt a first-in-first-out policy for readjustment. The supplier will change the customer's transport mode until a new demand–supply balance is reached, in which no customer has an incentive to change their route choice.

The service system assignment procedure is illustrated in Fig. 5. The service implementation involves the following steps: 1) Calculate the total commodities $f^{\tau u}_{i,j,t,t',k}$ at the pickup stage and obtain the attribute values $X^C_{w,\tau,u}$, $X^T_{w,\tau,u}$, and $X^F_{w,\tau,u}$ by adopting transport mode w at the transport stage. 2) Based on customers' route-choice behavior, the commodities $f^{\tau u}_{i,j,t,t',k_w}$ of different transport modes are generated at the transport stage. Owing to public vehicle capacity limitation, part of the commodities $f^{\tau u}_{i,j,t,t',k_3}$ must be readjusted to other transport modes. We considered the part of the commodities transported using trailer trucks in this study. 3) Based on the commodities $f^{\tau u}_{i,j,t,t',k_w}$ of different transport modes, the cost and time in the transport and delivery stages can be obtained. 4) Finally, the total generalized costs are output and demand–supply balance is achieved.

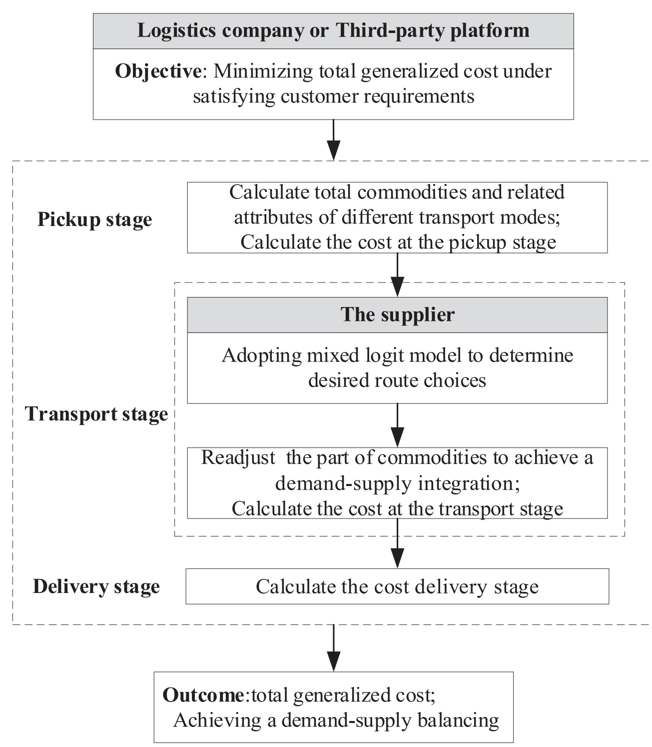

Fig. 5. Procedure for the service system assignment.

4. Adaptive large neighborhood search algorithm

The ALNS was developed to solve the proposed model. ALNS is known for its efficacy in routing and scheduling problems (Ropke &

Pisinger, 2006) and has been applied frequently to two-echelon vehicle routing problems, largely due to the freedom to finetune the algorithm (Hemmelmayr et al., 2012; Grangier et al., 2016; Jie, Yang, Zhang, & Huang, 2019). Unlike large neighborhood search (LNS) (Shaw, 1998), which only applies one destroy and one repair operator, ALNS considers multiple destroy and repair operators. ALNS works from an initial solution and iteratively applies a set of destroy and repair operators to improve the initial solution until a predefined number of iterations is reached. In each iteration of the ALNS algorithm, a destroy–repair pair is selected from the available operators, and a roulette-wheel mechanism is utilized. The probability of selecting the destroy–repair pair is assigned based on the corresponding weights, which depend on the historical performance of each operator. The value of each weight is initially set to be equal and then adjusted at each iteration. The newly generated solution is accepted based on a simulated annealing criterion. Utilizing different destroy and repair operators for different problems, and even for the same problem, varies in degrees of success. Fig. 6 shows a flowchart of the ALNS algorithm used in this study.

Compared with the classical ALNS, our proposed ALNS algorithm considers the following modifications: (1) In addition to optimizing vehicle distribution routes, the framework of the proposed ALNS algorithm can also determine the commodities for different transport modes to achieve a demand–supply balance in city logistics. (2) Some modifications on the destroy and repair operators are made to adapt the characteristics of the MCM-2E-VRP, including the consideration of store properties and scheduled time. (3) Unlike the adaptive mechanism illustrated in Ropke and Pisinger (2006), this study set the multiple sets of constants σ_1, σ_2, and σ_3 to calculate the score of the operator π according to the gap value between current and optimal solutions.

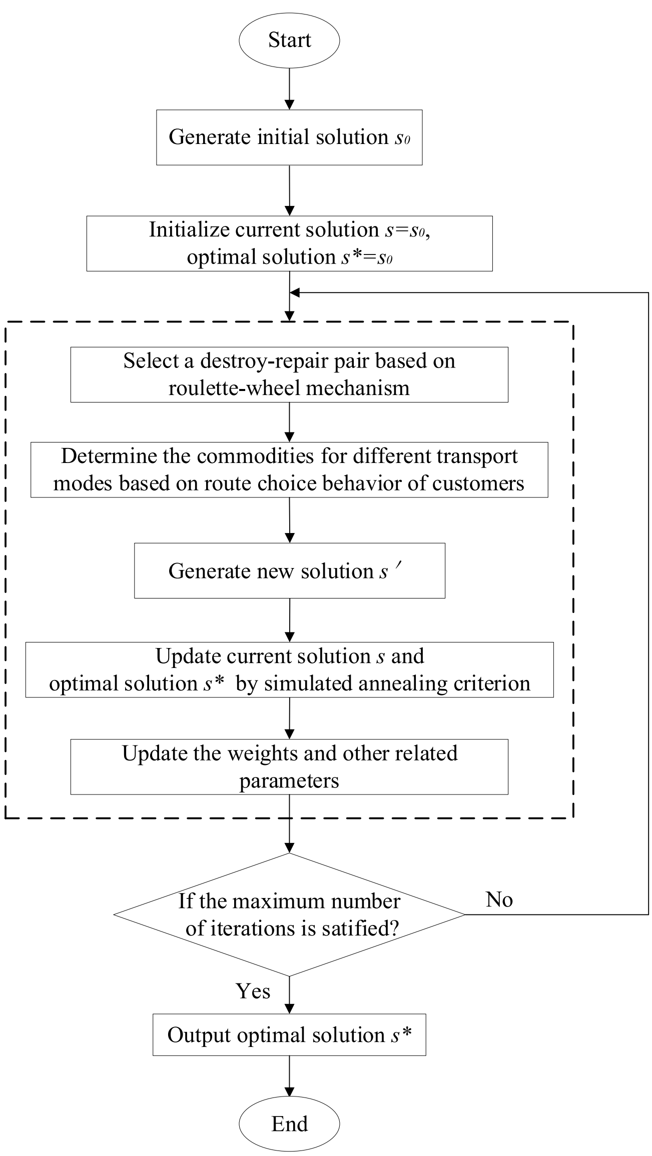

Fig. 6. Flowchart of the ALNS algorithm.

Our ALNS algorithm was customized as follows.

(1) Initial feasible solution:

The MCM-2E-VRP is divided into three stages: pickup, transport, and delivery. Accordingly, an initial feasible solution is generated based on a heuristic method consisting of three steps.

First, all stores are individually inserted into newly generated routes under vehicle capacity constraints. We can obtain the total commodities and costs at the pickup stage.

Next, a mixed logit model is applied to determine the commodities in the three transport modes. The commodities of the three transport modes can be readjusted based on the capacity constraints. The commodities in the three transport modes have different transport times, and the total cost of each transport mode in the transport stage can be determined.

Finally, all commodities are delivered to communities. We can obtain the total generalized costs and achieve a demand–supply balance. The generated initial solution satisfies all constraints, although the solution may be large.

(2) Process of the ALNS algorithm

The basic steps of the ALNS algorithm are presented in **Algorithm 1**. Given an initial feasible solution s_0 using a heuristic method, the iterations continue to improve it until the termination condition is reached. At each iteration, a destroy operator is used to remove part of the stores and a repair operator is then chosen to insert these stores back into current solution s to generate a new solution s'. A destroy–repair pair is selected using the roulette-wheel mechanism, and the commodities for the different transport modes are determined by applying a mixed logit model. The simulated annealing criterion is utilized to determine whether the newly generated solution s' can be accepted. If the objective function of the new solution s' is less than that of the current solution s, the new solution s' is considered acceptable. Otherwise, s' is accepted based on a probability function $e^{-(f(s')-f(s))/T}$, where T represents the current temperature. The initial temperature $T_0 = \delta f(s_0), \delta \in (0,1)$ and is updated via the formula $T = T_0 \times c^{\alpha}$, where the cooling rate $c \in (0,1)$.

Algorithm 1 Basic steps of the ALNS algorithm

Input: Iterations of each optimization phase φ, number of optimization phases γ, destroy operators D, repair operators I, cooling rate c, reaction factor η

Output: A best solution s^*

Obtain initial feasible solution s_0 using a heuristic method

Initialize best solution $s^* = s_0$, current solution $s = s_0$, $\gamma = 0$, $\alpha = 0$, $T_0 = \delta f(s_0)$, $\delta \in (0,1)$

Repeat

Initialize $\gamma := \gamma + 1$, $n = 0$

While $n < \varphi$, **do**

Use the roulette-wheel mechanism $\frac{w_d}{\sum_{j=1}^{|D|} w_j}, \frac{w_i}{\sum_{j=1}^{|I|} w_j}$ to select and apply a destroy–repair pair

Applying a mixed logit model to determine the commodities for different transport modes

If $f^{\tau u}_{i,j,t,t',k_w} \le Q^T_w$ then

Generating a new solution s'

Else

Adopting a first-in-first-out policy to readjust commodities $f^{\tau u}_{i,j,t,t',k_w}$ to achieve $f^{\tau u}_{i,j,t,t',k_w} \le Q^T_w$

Generating a new solution s'

If $f(s') < f(s^*)$ then

$s^* = s = s'$, update the score with σ_1

Else if $f(s') < f(s)$ then

$s = s'$, update the score with σ_2

Else if s' is accepted by probability function $e^{-(f(s')-f(s))/T}$

(*continued on next page*)

(*continued*)

$s = s'$, update the score with σ_3
End if
$n := n + 1$
Adjusting weights w_d, w_i, $d \in D, i \in I$
$T = T_0 \times c^{\alpha}$
If the number of iterations reaches φ,
Reset the weights $w_d = 1, w_i = 1$, $d \in D, i \in I$
$\alpha := \alpha + 1$
Until the predefined number of iterations is reached
Return best solution s^*

(3) Destroy operators

We use five destroy operators including random removal, worst removal, shaw removal, route removal, and route redistribution, which can be found in Ropke and Pisinger (2006; 2006) and Hemmelmayr et al. (2012). By applying these destroy operators, the predetermined stores are removed from the current solution s and saved to the removal list L_r. The structure of the destroy operators is presented as **Algorithm 2** in Appendix A.

Random removal: The random removal operator simply selects a predetermined number of stores at random and adds them into the removal list L_r.

Worst removal: The worst removal operator is adapted to remove the predetermined number of stores with the maximum improvement in the objective value. The removal cost for each store is defined as the difference between the objective values of the distribution routes with and without the store.

Shaw removal: The shaw removal operator is designed to remove the predetermined number of stores with similar relatedness. The concept of similar relatedness consists of the transport distance between two store nodes i and j, the pickup time of each store node, and the number of commodities of each store, described as $SC(i,j) = \mu_1 d_{ij} + \mu_2 |t_i - t_j| + \mu_3 |q_i - q_j|$, where μ_1, μ_2, and μ_3 are normalized weights.

Route removal: The route removal operator is used to remove stores on the route with the longest distribution time and place them on the removal list L_r.

Route redistribution: The route redistribution operator is adapted to remove stores on three routes with the minimum distance between the satellite to which it is assigned and any other satellite.

(4) Repair operators

Two repair operators consisting of greedy and k-regret insertions are used, which can be found in Ropke and Pisinger (2006; 2006). After applying the destroy operators, the removal store nodes must be reinserted into the partial solution s_p. The repair operations ensure the feasibility of generating a new solution s' and improves its quality. The structure of the repair operators is presented as **Algorithm 3** in Appendix A.

Greedy insertion: The greedy insertion operator calculates the insertion cost of inserting each store into all feasible insertable positions and reinserts the store into its best position with the minimum insertion cost.

K-regret insertion: By considering a look-ahead concept, the k-regret insertion operator is used to calculate the gap between the minimum insertion cost and the kth minimum insertion cost of each store from removal list L_r. The operator then selects the store with the greatest gap and inserts it into the corresponding position.

(5) Adaptation mechanism

The adaptive mechanism was designed to improve the performance of operators during the destroy and repair operations. **Algorithm 1** uses the roulette-wheel mechanism to select destroy and repair operations. The weight of each operator is initialized to 1 when the algorithm starts. At each iteration, a destroy–repair pair is selected based on the probabilities $\frac{w_d}{\sum_{j=1}^{|D|} w_j}$ and $\frac{w_i}{\sum_{j=1}^{|I|} w_j}$. Then, in each optimization phase, the weights are adjusted via the formulas $w_d^{n+1} = w_d^n(1-\eta) + \eta\pi_{dn}/\theta_{dn}$, and $w_i^{n+1} = w_i^n(1-\eta) + \eta\pi_{in}/\theta_{in}$, where $\eta \in [0,1]$ is defined as the reaction factor, θ denotes the number of times the operator is used, and π is the score of the operator. Furthermore, π is updated by the constants σ_1, σ_2, and σ_3, where σ_1: a best new solution is obtained, σ_2: a new solution is better than the current solution, and σ_3: a new solution is accepted by the simulated annealing criterion.

5. Computational experiments

The numerical experiments are described in this section. Section 5.1 describes the verification of the efficiency of the model and ALNS algorithm. Section 5.2 presents the computational results of the experiments with the model on the realistically sized Beijing Yizhuang transportation network, assessing the performance of the proposed solution, including a sensitivity analysis. The model and solution approaches were coded in Python, and all experiments were conducted on a single thread 2.60 GHz Intel(R) Core (TM) I7 processor with 32 GB RAM.

5.1. Case study

5.1.1. Performance in solving 2E-VRP benchmark instances

We validated the quality of our proposed model and the ALNS algorithm by solving the small 2E-VRP benchmark instances, because the 2E-VRP is a special case of the MCM-2E-VRP. The small 2E-VRP benchmark instances including "set-2" and "set-3" were obtained from Breunig, Schmid, Hartl, and Vidal (2016). We used Gurobi to solve the proposed model within a time limit of 7200 s. To solve the 2E-VRP instances to optimality, the gap value was set to zero. If Gurobi could not find optimal solutions within the maximum time, we obtained the upper bound at the end of the time limit. Before adopting the ALNS algorithm, several benchmark instances were randomly selected for parameter tuning to determine the best combination of parameters. The final parameter values were set as follows: the number of worst removals was within (Belgin et al., 2018; Cuda et al., 2015), the route redistribution number was set to 1, the coefficient of regret-n was 2, and the other parameter values were the same as those in Table B1 in Appendix B. Tables 3 and 4 summarize the results for set-2 and set-3 of the 2E-VRP benchmark instances. The first column represents the benchmark instance. The second column lists the best-known solution (BKS) of the benchmark instances. The BKS solutions were obtained from Breunig et al. (2016). The next three columns show the best solution (either optimal solutions or upper bounds), computation time, and gap to the BKS of the mathematical model. The last three columns show the best solution, the computation time when the optimal solution is obtained, and the gap to the BKS of the ALNS algorithm.

From Tables 3 and 4, we can see that Gurobi obtained optimal solutions in 12 out of 30 instances in set-2 and 9 out of 24 instances in set-3. Specifically, Gurobi solved all instances with 22 customers to optimality, and the average gap for all set-2 instances was 1.12 %. Similarly, all instances with 22 customers in set-3 were also optimal, and the average gap for all set-3 instances was less than 1 %. We further tested the 2c and 3c instances compared with those of Kancharla and Ramadurai (2019), and the average gaps of the set-2 and set-3 instances were reduced from 2.34 % and 2.52 % to 1.12 % and 0.97 %, respectively. Furthermore, the ALNS algorithm obtained the optimal solutions for the set-2 and set-3 instances based on Tables 3 and 4, which are the same as the results of Hemmelmayr et al. (2012), Breunig et al. (2016), and Vincent et al. (2023). In addition, the designed ALNS algorithm employed the maximum number of iterations and presented only the time required to obtain an optimal solution. The computation times were generally consistent with those of other well-performing heuristics. Therefore, we conclude that the proposed model and ALNS algorithm can effectively solve the small 2E-VRP benchmark instances.

Table 3
Results for set-2 of the 2E-VRP benchmark instances.

Instance	BKS	Mathematical model			ALNS algorithm		
		Best	t (s)	Gap (%)	Best	t (s)	Gap (%)
Set 2a							
E-n22-k4-s6-17	417.07	417.07	6	0	417.07	1	0
E-n22-k4-s8-14	384.96	384.96	27	0	384.96	1	0
E-n22-k4-s9-19	470.60	470.60	44	0	470.60	1	0
E-n22-k4-s10-14	371.50	371.50	6	0	371.50	1	0
E-n22-k4-s11-12	427.22	427.22	92	0	427.22	2	0
E-n22-k4-s12-16	392.78	392.78	24	0	392.78	1	0
E-n33-k4-s1-9	730.16	730.16	937	0	730.16	3	0
E-n33-k4-s2-13	714.63	714.63	385	0	714.63	4	0
E-n33-k4-s3-17	707.48	707.48	439	0	707.48	3	0
E-n33-k4-s4-5	778.74	800.73	7200	2.82	778.74	4	0
E-n33-k4-s7-25	756.85	756.85	761	0	756.85	4	0
E-n33-k4-s14-22	779.05	779.05	417	0	779.05	3	0
Set 2b							
E-n51-k5-s2-4-17-46	530.76	537.43	7200	1.26	530.76	17	0
E-n51-k5-s2-17	597.49	602.42	7200	0.83	597.49	12	0
E-n51-k5-s4-46	530.76	530.76	2452	0	530.76	9	0
E-n51-k5-s6-12	554.81	558.79	7200	0.72	554.81	13	0
E-n51-k5-s6-12-32-37	531.92	532.98	7200	0.20	531.92	16	0
E-n51-k5-s11-19	581.64	587.59	7200	1.02	581.64	11	0
E-n51-k5-s11-19-27-47	527.63	529.49	7200	0.35	527.63	16	0
E-n51-k5-s27-47	538.22	576.48	7200	7.11	538.22	15	0
E-n51-k5-s32-37	552.28	570.84	7200	3.36	552.28	14	0
Set 2c							
E-n51-k5-s2-4-17-46	601.39	605.13	7200	0.62	601.39	14	0
E-n51-k5-s2-17	601.39	602.77	7200	0.23	601.39	13	0
E-n51-k5-s4-46	702.33	713.41	7200	1.58	702.33	13	0
E-n51-k5-s6-12	567.42	586.36	7200	3.34	567.42	11	0
E-n51-k5-s6-12-32-37	567.42	585.45	7200	3.18	567.42	15	0
E-n51-k5-s11-19	617.42	633.71	7200	2.64	617.42	14	0
E-n51-k5-s11-19-27-47	530.76	537.43	7200	1.26	530.76	12	0
E-n51-k5-s27-47	530.76	544.21	7200	2.53	530.76	12	0
E-n51-k5-s32-37	752.59	755.67	7200	0.41	752.59	13	0
Average	578.27	584.8	4506	1.12	578.27	9	0

5.1.2. Performance in solving MCM-2E-VRP instances

Because the MCM-2E-VRP is a new problem, no benchmark instances exist. We designed the newly generated MCM-2E-VRP instances on physical networks available at https://github.com/Datainstances/MCM-2E-VRP-instances.git. We obtained solutions to the MCM-2E-VRP instances by solving the mathematical model shown in Section 3.3 via Gurobi and the ALNS algorithm. The maximum time for Gurobi was set to 7200 s. We mark the instances where Gurobi meets out of memory with a "—." The parameter values of the ALNS algorithm were the same as those described in Section 5.1.1. Table 5 lists the computational results obtained by Gurobi and ALNS for the MCM-2E-VRP instances. The first column provides information about the instances, including the number of stores ($|S|$), communities ($|C|$), and periods ($|P|$). The second and third columns represent the total generalized costs and the corresponding computation times obtained by Gurobi. The next two columns report the total generalized costs and computation times obtained by ALNS. The final column shows the cost gap between the Gurobi and ALNS methods.

Table 4
Results for set-3 of the 2E-VRP benchmark instances.

Instance	BKS	Mathematical model			ALNS algorithm		
		Best	t (s)	Gap (%)	Best	t (s)	Gap (%)
Set 3a							
E-n22-k4-s13-14	526.15	526.15	82	0	526.15	2	0
E-n22-k4-s13-16	521.09	521.09	131	0	521.09	2	0
E-n22-k4-s13-17	496.38	496.38	152	0	496.38	3	0
E-n22-k4-s14-19	498.80	498.80	178	0	498.80	1	0
E-n22-k4-s17-19	512.81	512.81	247	0	512.81	4	0
E-n22-k4-s19-21	520.42	520.42	337	0	520.42	2	0
E-n33-k4-s16-22	672.17	676.80	7200	0.69	672.17	4	0
E-n33-k4-s16-24	666.02	666.02	674	0	666.02	3	0
E-n33-k4-s19-26	680.37	680.37	1522	0	680.37	3	0
E-n33-k4-s22-26	680.37	680.37	1352	0	680.37	3	0
E-n33-k4-s24-28	670.43	678.29	7200	1.17	670.43	3	0
E-n33-k4-s25-28	650.58	665.75	7200	2.33	650.58	4	0
Set 3b							
E-n51-k5-s12-18	690.59	718.16	7200	3.99	690.59	14	0
E-n51-k5-s12-41	683.05	702.52	7200	2.85	683.05	10	0
E-n51-k5-s12-43	710.41	711.03	7200	0.09	710.41	11	0
E-n51-k5-s39-41	728.54	740.65	7200	1.66	728.54	13	0
E-n51-k5-s40-41	723.75	742.57	7200	2.60	723.75	12	0
E-n51-k5-s40-43	752.15	766.43	7200	1.90	752.15	16	0
Set 3c							
E-n51-k5-s13-19	560.73	574.57	7200	2.47	560.73	12	0
E-n51-k5-s13-42	564.45	565.06	7200	0.11	564.45	18	0
E-n51-k5-s13-44	564.45	565.06	7200	0.11	564.45	15	0
E-n51-k5-s40-42	746.31	752.45	7200	0.82	746.31	10	0
E-n51-k5-s41-42	771.56	777.08	7200	0.72	771.56	12	0
E-n51-k5-s41-44	802.91	816.28	7200	1.67	802.91	13	0
Average	641.44	648.13	4695	0.97	641.44	8	0

Table 5
Computational results of Gurobi and the ALNS algorithm.

Instances$\|S\|-\|C\|-\|P\|$	Gurobi		ALNS		Gap (%)
	Cost (unit)	t (s)	Cost (unit)	t (s)	
2-2-1	91	31	91	1	0
2-2-2	186	67	186	1	0
2-2-3	273	98	273	1	0
2-2-4	380	137	380	2	0
2-2-5	463	170	463	3	0
2-2-6	554	204	554	4	0
2-2-7	637	240	637	5	0
2-2-8	736	275	736	7	0
2-2-9	819	312	819	8	0
2-2-10	926	344	926	10	0
4-2-1	108	37	108	1	0
4-2-2	216	79	216	1	0
4-2-3	324	118	324	2	0
4-2-4	432	155	432	4	0
4-2-5	540	196	540	5	0
4-2-6	644	234	644	8	0
4-2-7	756	281	756	10	0
4-2-8	856	313	856	11	0
4-2-9	972	347	972	11	0
4-2-10	1080	394	1080	12	0
6-3-1	133	154	133	1	0
6-3-2	266	317	266	1	0
6-3-3	391	478	391	3	0
6-3-4	532	647	532	5	0
6-3-5	665	810	665	7	0
6-3-6	794	984	794	10	0
6-3-7	919	1139	919	13	0
6-3-8	1064	1336	1064	15	0
6-3-9	—	—	1193	19	—
6-3-10	—	—	1318	21	—

As shown in Table 5, 28 of the 30 small MCM-2E-VRP instances were solved to optimality by Gurobi. The computation time gradually increased with the problem size, and Gurobi ran out of memory when solving instances 6–3-9 and 6–3-10. For each optimal solution, ALNS provided the same solution within 20 s. For instances 6–3-9 and 6–3-10, ALNS still obtained the solution within approximately 20 s. In terms of computation time, ALNS outperformed the exact Gurobi method for small-scale MCM-2E-VRP instances. While Gurobi required 1336 s to solve the 6–3-8 instance, ALNS only needed15 s. ALNS obtained optimal solutions for all small instances with a significantly lower computational time than Gurobi. Therefore, we utilized ALNS to solve large-scale instances, as described in Section 5.2.

5.1.3. Analysis of user heterogeneity for the MCM-2E-VRP

As shown in this section, we analyzed two approaches, (1) the MCM-2E-VRP and (2) MCM-2E-VRP, considering user heterogeneity in the MCM-2E-VRP instances in Section 5.1.2. The MCM-2E-VRP determines which transport mode is selected based solely on total costs, whereas the MCM-2E-VRP considers user heterogeneity by using a discrete choice model to capture user heterogeneity for multimodal transport in terms of distribution time and total costs. The analyses were conducted based on the solutions provided by Gurobi. We measured two indicators, distribution time and total costs, to compare the two approaches. Table 6 summarizes the results of the analyses. The first column presents the instances. The next five columns provide information on the MCM-2E-VRP. In the MCM-2E-VRP instances, it was assumed that the capacities of the trailer trucks and public vehicles were sufficient. Because this MCM-2E-VRP considers the total cost as the objective function, rigid transport with high cost and short time attributes was not used. The last few columns provide information on the MCM-2E-VRP considering user heterogeneity, including commodities, distribution time of the three transport modes, and total costs.

As shown in Table 6, by considering user heterogeneity in the MCM-2E-VRP, some commodities could be delivered earlier by rigid trucks than by trailer trucks or public vehicles when time is the primary objective of customers. Without considering user heterogeneity, commodities were distributed by trailer trucks and public vehicles to minimize total costs. For example, in the 4–2-1 instance, commodities of [3;2] were delivered to the corresponding customers via rigid trucks

Table 6
Analysis of user heterogeneity for the MCM-2E-VRP.

Instances	MCM-2E-VRP					MCM-2E-VRP considering user heterogeneity						
	Trailer transport		Public transport		Total cost	Rigid transport		Trailer transport		Public transport		Total cost
	Commodities	t (min)	Commodities	t (min)		Commodities	t (min)	Commodities	t (min)	Commodities	t (min)	
2-2-1	[3;4]	76	[0;2]	80	61	[1;1]	59	[2;3]	76	[0;2]	80	91
2-2-2	[8;6]	76	[2;1]	80	126	[2;2]	59	[6;4]	76	[2;1]	80	186
2-2-3	[8;10]	76	[2;3]	80	183	[2;3]	55	[6;7]	76	[2;3]	80	273
2-2-4	[13;16]	76	[4;5]	84	260	[4;5]	59	[9, 11]	76	[4;5]	84	380
2-2-5	[16;19]	76	[2;6]	80	313	[5;6]	59	[11;13]	76	[2;6]	80	463
2-2-6	[18;23]	76	[5;5]	80	374	[5;7]	55	[13;16]	76	[5;5]	80	554
2-2-7	[24;19]	76	[6;3]	80	427	[8;5]	55	[16;14]	76	[6;3]	80	637
2-2-8	[30;26]	76	[5;7]	80	496	[9;7]	55	[21;19]	76	[5;7]	80	736
2-2-9	[29;32]	76	[6;5]	80	549	[7;10]	55	[22;22]	76	[6;5]	80	819
2-2-10	[32;32]	76	[7;9]	80	626	[9;9]	55	[23;23]	76	[7;9]	80	926
4-2-1	[6;6]	72	[2;2]	84	83	[3;2]	59	[3;4]	76	[2;2]	84	108
4-2-2	[14;11]	72	[4;4]	84	166	[7;4]	59	[7;7]	76	[4;4]	84	216
4-2-3	[21;16]	72	[5;5]	84	249	[9;6]	59	[12;10]	76	[5;5]	84	324
4-2-4	[24;23]	72	[5;8]	84	332	[9;9]	59	[15;14]	76	[5;8]	84	432
4-2-5	[29;27]	72	[7;8]	84	406	[12;10]	59	[17;17]	76	[7;8]	84	540
4-2-6	[29;37]	72	[8;11]	80	494	[11;15]	59	[18;22]	76	[8;11]	80	644
4-2-7	[42;39]	72	[10;13]	84	563	[17;16]	59	[25;23]	76	[10;13]	84	756
4-2-8	[48;44]	72	[12;10]	80	656	[19;17]	59	[29;27]	76	[12;10]	80	856
4-2-9	[60;47]	72	[20;15]	84	747	[26;18]	59	[34;29]	76	[20;15]	84	972
4-2-10	[56;62]	72	[19;18]	84	830	[21;26]	59	[35;36]	76	[19;18]	84	1080
6-3-1	[4;4;5]	76	[1;1;1]	88	104	[1;1;2]	63	[3;3;3]	80	[1;1;1]	88	133
6-3-2	[6;10;8]	76	[2;4;2]	88	208	[2;4;2]	63	[4;6;6]	80	[2;4;2]	88	266
6-3-3	[11;13;16]	76	[4;3;5]	84	304	[4;4;6]	59	[7;9;10]	80	[4;3;5]	84	391
6-3-4	[18;17;21]	76	[6;5;6]	88	420	[6;5;8]	63	[12;12;13]	80	[6;5;6]	88	532
6-3-5	[21;24;18]	76	[6;6;5]	88	520	[6;8;6]	63	[15;16;12]	80	[6;6;5]	88	665
6-3-6	[32;32;29]	76	[10;9;7]	84	624	[13;12;11]	63	[19;20;18]	80	[10;9;7]	84	794
6-3-7	[32;24;31]	76	[8;7;8]	80	716	[11;6;10]	59	[21;18;21]	80	[8;7;8]	80	919
6-3-8	[31;34;32]	76	[11;9;9]	88	832	[10;11;11]	63	[21;23;21]	80	[11;9;9]	88	1064

within one hour, but the total cost increased from 83 to 108 units. By modeling user heterogeneity, the supplier can choose a suitable transport mode to deliver commodities based on the attributes of the transport modes to capture customer requirements.

5.2. Tests using the real-world Beijing Yizhuang transportation network

5.2.1. Transportation network and parameter setting

The transportation network of Beijing Yizhuang is shown in Fig. 7. It consists of 1954 nodes and 4807 links. The datasets are available at https://github.com/Datainstances/Beijing_YiZhuang_network.git. The network comprises four satellites. Each satellite has a sufficient capacity to process and store data. We generated shipping services on predefined lines between the two satellites, as shown in Fig. 7. Three transport modes–rigid trucks, trailer trucks, and public vehicles–were allowed to travel on each transport line. Seven communities were generated for distribution, and stores were randomly generated. Each store also randomly generated commodities from seven communities [3, 2, 0, 3, 0, 1, 2]. We considered a planning horizon divided into 10 periods of 3 h each. The time window for each shipment was generated in the space–time network. The service time of stores and communities was set to 2 min, and the transfer time at the satellite facilities was assumed to be 5 min.

The settings of the three transport modes (rigid trucks, trailer trucks, and public vehicles) were as follows: The travel costs of the three transport modes were set to 4, 2, and 1 units/km, respectively, and their fixed costs were 20, 30, and zero units, respectively. The capacities of the three transport modes were 50, 100, and random units. We considered the fixed cost of public vehicles to be zero, and the capacity of public vehicles to be randomly generated. The capacity of public vehicles in the first and last periods was assumed to lie within (Kim et al., 2023; Shaw, 1998) and the capacity in other periods within [40, 60]. The average velocities of the three transport modes were set to 54, 42, and 30 km/h, respectively. In the pickup and delivery stages, the travel cost, fixed cost, capacity, and average velocity of the SE vehicles were 1 unit/km, 10 units, 30 units, and 24 km/h, respectively. As expected, the instances generated in the transportation network were too large for the standard Gurobi solver, and we adopted ALNS as described above. The parameters used are listed in Table B1 of Appendix B.

5.2.2. Analysis of the results

Next, we designed five scenarios, and 24 instances of each scenario were generated with different stores and commodities, where the number of stores varied from 282 to 568, and the number of commodities varied from 2833 to 5826. For each instance, the best solution from five repeated experiments was adopted. A maximum of 500 iterations was imposed for all instances. The run time increased significantly from 1 h to approximately 10 h with the size of the instances. The five scenarios were:

(1) **Basic scenario**. Considering the heterogeneity of users, there are three stages in the MCM-2E-VRP: the transport stage in the first echelon and the pickup and delivery stages in the SE. In the pickup stage, the SE vehicles perform pickup operations at randomly generated stores. Three transport modes–rigid trucks, trailer trucks, and public vehicles–can be selected to transport commodities by considering the heterogeneity of users during the transport stage. Owing to the different transport times of the three modes, the commodities are distributed by the three groups of SE vehicles in the delivery stage. For convenience, the commodities of

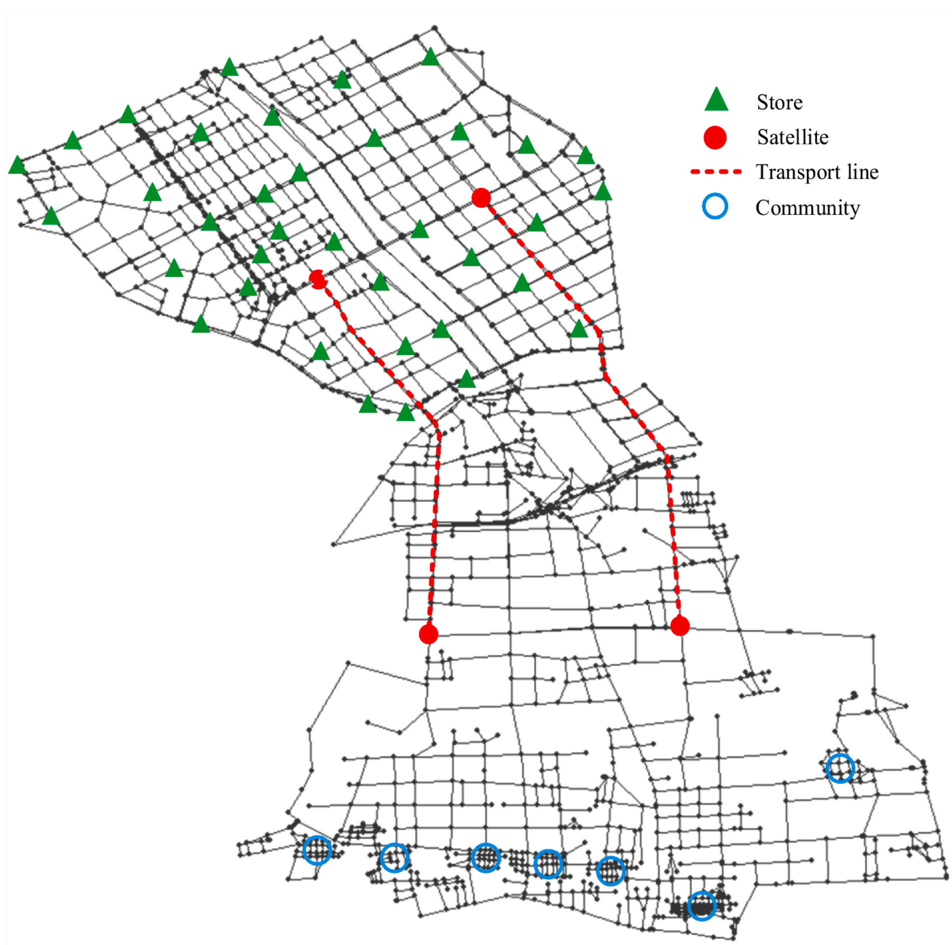

Fig. 7. Beijing Yizhuang Transportation Network.

the rigid trucks, trailer trucks, and public vehicles are referred to as rigid, trailer, and public commodities, respectively.

(2) **Scenario I**. The multimodal service including rigid trucks, trailer trucks, and public vehicles is still adopted to transport commodities in the transport stage. However, the heterogeneity of users will not be considered, that is, all commodities are uniformly delivered to communities during the delivery stage. The remaining configuration is the same as in the Basic scenario.

(3) **Scenario II**. One service modal (rigid trucks) is allowed to transport commodities in the transport stage, and the remaining settings are the same as in Scenario I.

(4) **Scenario III**. Only trailer trucks are used to transport commodities in the transport stage, and the remaining configuration is the same as in Scenario I.

(5) **Scenario IV**. Only public vehicles are adopted to transport commodities in the transport stage, and the remaining settings are the same as in Scenario I.

For the Basic scenario, we analyzed the cost per stage behavior of two main variables: the number of stores and number of commodities. The computational results for the Basic scenario are presented in Table C1 in Appendix C. The following information can be obtained: (1) Cost at each stage. Considering the heterogeneity of users, three transport modes were selected, and three groups of SE vehicles delivered the commodities. Thus, three types of travel and fixed costs were formed in the transport and delivery stages according to the three transport modes. Moreover, the cost at each stage generally increased with the number of stores and commodities. (2) Demand–supply balancing. Public vehicles transported commodities with only the remaining capacity. Owing to capacity limitations, some public commodities were delivered using trailer trucks. The fixed costs of public vehicles were not considered in this study. Thus, the travel cost C_7 of public vehicles remained unchanged. The detailed results for instance B_12 are listed in Table C2, showing the commodities to seven communities of three transport modes and the costs at different stages in each period. The results of the Basic scenario reveal that the MCM-2E-VRP considering user heterogeneity can be effectively solved using the proposed solution.

To evaluate the impact of user heterogeneity, we constructed the instances of Scenario I, and the computational results are listed in Table C3. We used two performance indicators for comparison: the number of SE vehicles and the cost during the delivery stage. The comparison results are shown in Fig. 8. As shown, the cost and number of vehicles in the delivery stage when considering user heterogeneity were, on average, 1350 and 43 higher, respectively, than those without consideration. In other words, the supplier must allocate four more vehicles in each period, resulting in an additional cost of 135 units to satisfy the customer requirements. Furthermore, the three groups of SE vehicles delivered commodities owing to the different transport times of the three transport modes in the Basic scenario. Among them, the earliest starting delivery time of SE vehicles was for the delivery of rigid commodities, followed by trailer commodities and then public commodities. In Scenario I, commodities were delivered uniformly, and the start time of unified distribution was regarded as the starting delivery time of public commodities by SE vehicles in the Basic scenario. As shown in Fig. 9, SE vehicles for rigid and trailer commodities, accounting for an average of 77.2 % of all SE vehicles in the Basic scenario, could deliver earlier than SE vehicles for public commodities and Scenario I. Therefore, although the heterogeneity of users increases the cost to the supplier, it better meets customer requirements from the perspective of time.

Furthermore, we analyzed the performance of multiple transport modes versus a single transport mode by constructing three single-mode scenarios (Scenario II, Scenario III, and Scenario IV). The results obtained for each transport mode are reported in Tables C4, C5, and C6 for rigid truck, trailer truck, and public transport, respectively. Fig. 10 summarizes the performance of the total generalized costs for the different scenarios. The cost variation trend for each scenario with the size of instances was the same, and the cost of multiple transport modes (Basic scenario and Scenario I) essentially fell between the cost of rigid trucks (Scenario II) and the cost of trailer trucks (Scenario III). The cost of public transport (Scenario IV) was the lowest. However, the remaining capacity of public vehicles is limited in real life, and they cannot deliver all commodities. In addition, although the time required to use rigid trucks to transport commodities was the lowest, the cost was relatively high. Therefore, a multimodal transport service with relatively moderate costs and the ability to satisfy diverse customer preferences in terms of time and cost can be applied as an urban logistics service.

5.2.3. Sensitivity analyses of city logistics service

As described in this section, we investigated the impact of store distribution and vehicle capacity on the solutions, including the cost and number of vehicles. To perform the sensitivity analysis, we varied only one parameter at a time. The maximum number of iterations per instance was set to 500. We first analyzed the impact of store distribu-

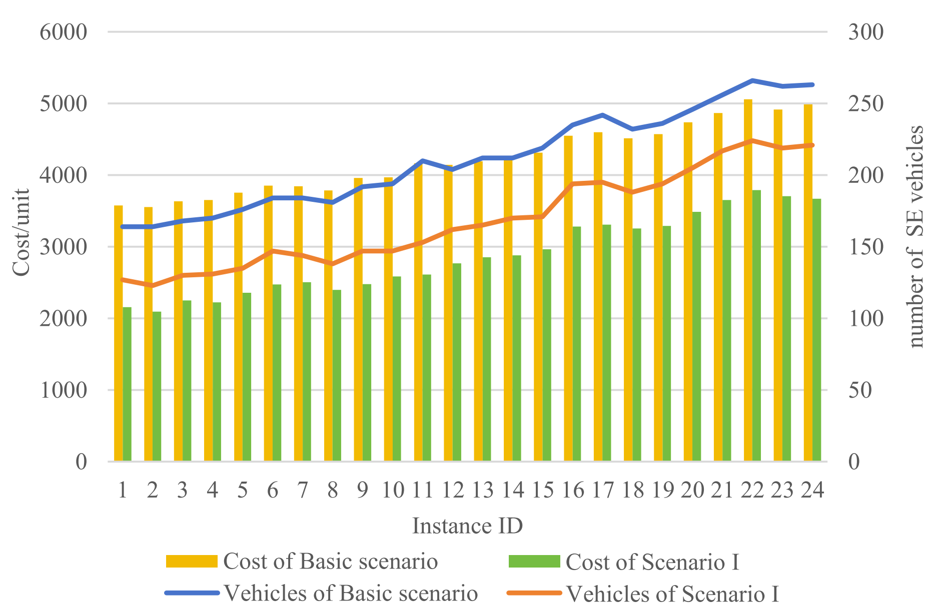

Fig. 8. Cost and vehicles in the delivery stage between the Basic scenario and Scenario I.

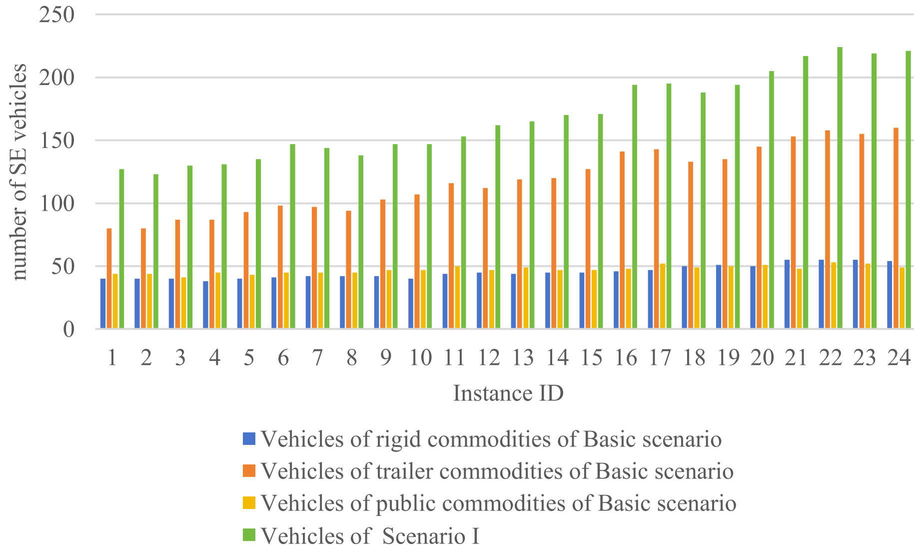

Fig. 9. Comparison of vehicles between the Basic scenario and Scenario I.

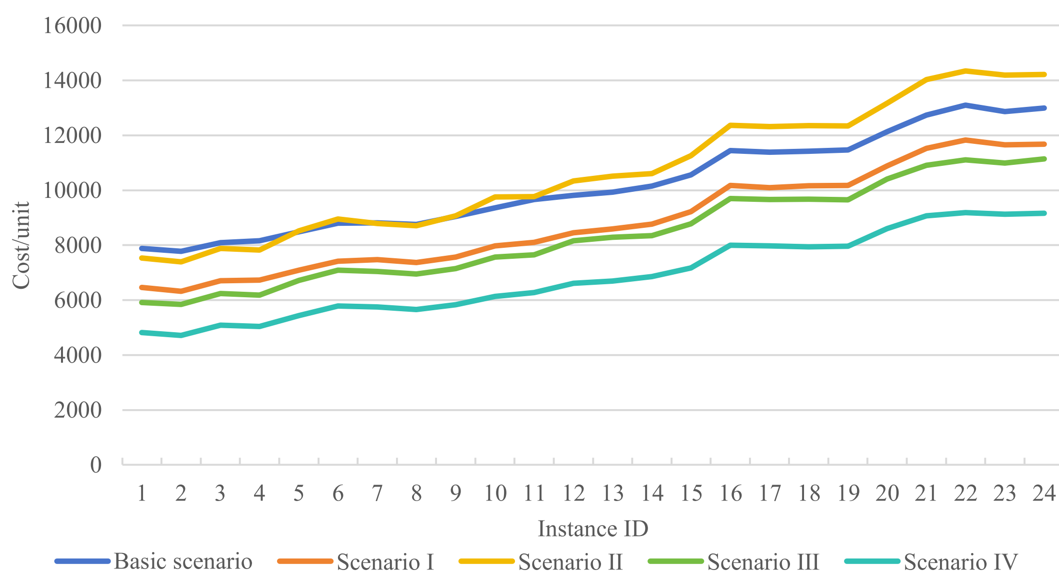

Fig. 10. Total generalized costs under different scenarios.

tions, including random and cluster distributions, for an identical number of stores and commodities, as shown in Fig. 11. Fig. 11 presents the two distributions of the 5th period for Instance R_C_10. In the random distribution, the store locations were randomly distributed in the pickup stage. However, store locations are generally not fairly distributed in urban areas; thus, we also created a cluster store distribution. In the cluster distribution, we generated two nonoverlapping areas of clusters. Each store was randomly located in the two clusters C_1, C_2 or in another random location, C_{ran}. The likelihood of a store selecting a location was $pC_1 = pC_2 = pC_{ran} = 1/3$. Forty instances were generated, and the computational results are summarized in Table C7. Because changes in store distributions only affect operations in the pickup stage, we present the cost and number of SE vehicles in the pickup stage based on the different distributions in Table C7. Fig. 12 shows the changes in the cost and number of SE vehicles. Compared with the random distribution, the cost of the cluster distribution could save 13.02 % on average, yet the number of SE vehicles used did not change significantly. Therefore, although the number of vehicles in the cluster distribution was essentially the same, the cost was reduced. Concentration and specialization are the primary methods for improving efficiency and reducing costs in the logistics industry (Liu, He, Cao, Li, & Jian, 2022). Thus, logistics services have the advantage of evolving into clusters.

We performed a further analysis on the impact of the capacity of vehicles consisting of SE vehicles, rigid trucks, and trailer trucks. Thus, we set three subsets of instances according to the varying capacity of the three vehicles and the Basic scenario with the capacity of the SE vehicle, rigid truck, and trailer truck was called C_30_50_100 for comparison purposes. All instances had the same store setting, including 408 stores and 4273 commodities. The computational results are presented in Table C8. Figs. 13, 14, and 15 show the changes in the cost and number of vehicles with different vehicle capacities, including those of SE vehicles, rigid trucks, and trailer trucks. The results show that with an increase in vehicle capacity, the cost of the corresponding stage and the number of vehicles required decreased accordingly. Not surprisingly, there was an inverse relationship between vehicle capacity and the number of vehicles. Furthermore, we observed that an increase in the capacity of rigid trucks had no impact on the cost or number of vehicles when the capacity was within [60,70]. This indicates that the capacity of rigid trucks is no longer a constraint that limits transport costs. Thus,

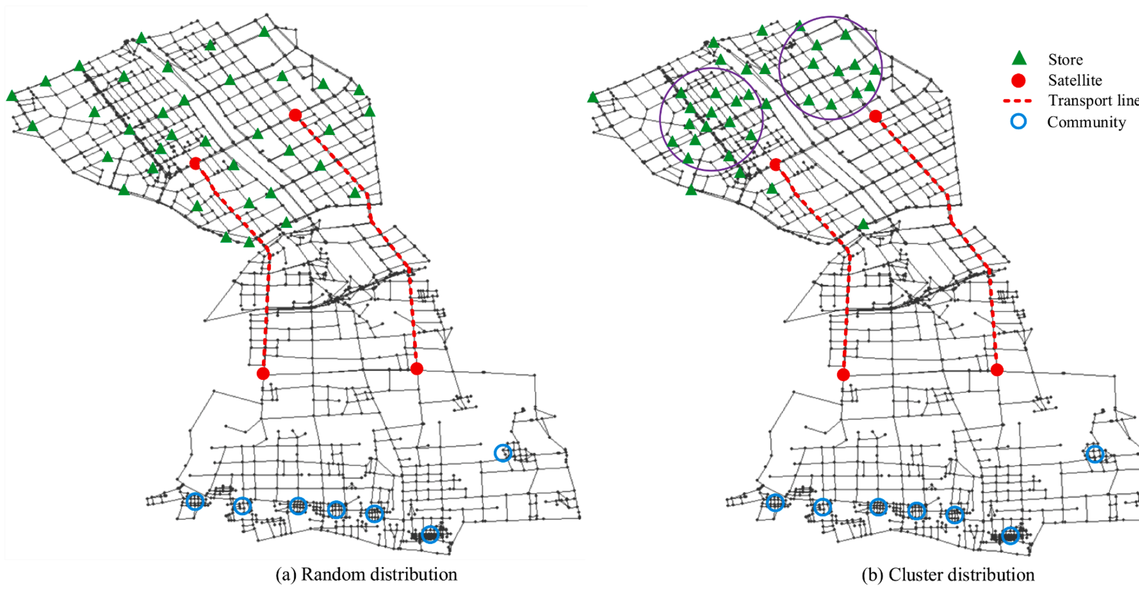

Fig. 11. Two store distributions: (a) random and (b) cluster distributions.

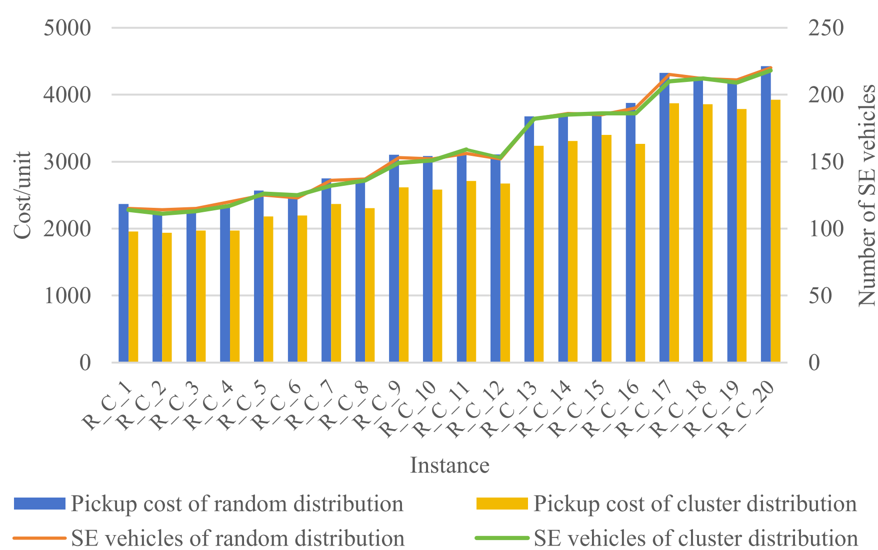

Fig. 12. Comparison of pickup cost and SE vehicles between the two distributions.

when the quantity of commodities is fixed, there is an inverse relationship between vehicle capacity and the number of vehicles. However, logistics companies do not recommend blindly increasing vehicle capacity to reduce the number of vehicles and transport costs, especially when it reaches a critical threshold.

6. Conclusions

In this study, we introduced the MCM-2E-VRP as a new extension of the 2E-VRP by considering multiple transport modes and commodities. Specifically, commodities can be transported by rigid trucks, trailer trucks, or public transport in the first echelon. To capture the heterogeneity of users, we used a random utility discrete choice model to allocate commodities. Furthermore, we applied a many-to-one logistics setting in which multiple commodities can be collected from any store, and customers can obtain their commodities in a multi-period horizon. The objective is to minimize the total generalized costs while satisfying customer requirements.

To address the MCM-2E-VRP, we divided this complex problem into three stages: pickup, transport, and delivery stages. Then, we formulated it as an integer linear programming model based on a space–time network, and the customers' route-choice behavior at the transport stage was modeled using a mixed logit model. Some public commodities must be readjusted to other transport modes because of public vehicle capacity limitations. To achieve a demand–supply balance, this study considered that some of the public commodities were transported using trailer trucks. We further introduced an ALNS algorithm to the model to allow the handling of large applications. Because the 2E-VRP is a special case of the MCM-2E-VRP, we validated the quality of our proposed model and the ALNS algorithm by solving the 2E-VRP benchmark instances. Furthermore, we assessed the performance of the proposed model and ALNS by solving newly generated MCM-2E-VRP instances and analyzing user heterogeneity for the MCM-2E-VRP.

Extensive numerical experiments were conducted using the Beijing Yizhuang transportation network. The studies revealed that compared to Scenario I, the Basic scenario considering user heterogeneity introduced an increase in the cost to the supplier; however, it better met the customers' requirements from the perspective of time. Moreover, by

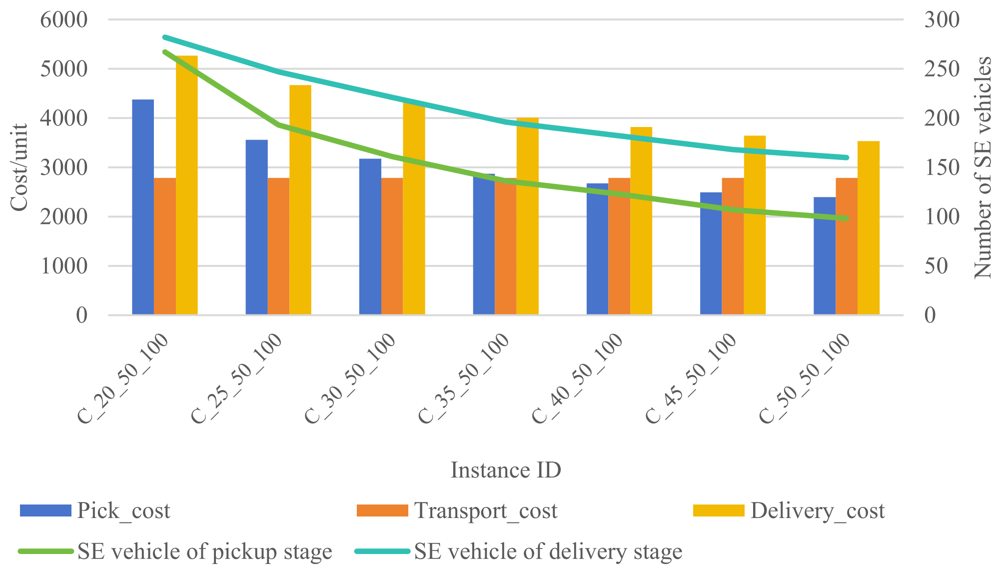

Fig. 13. Impact of SE vehicle capacity.

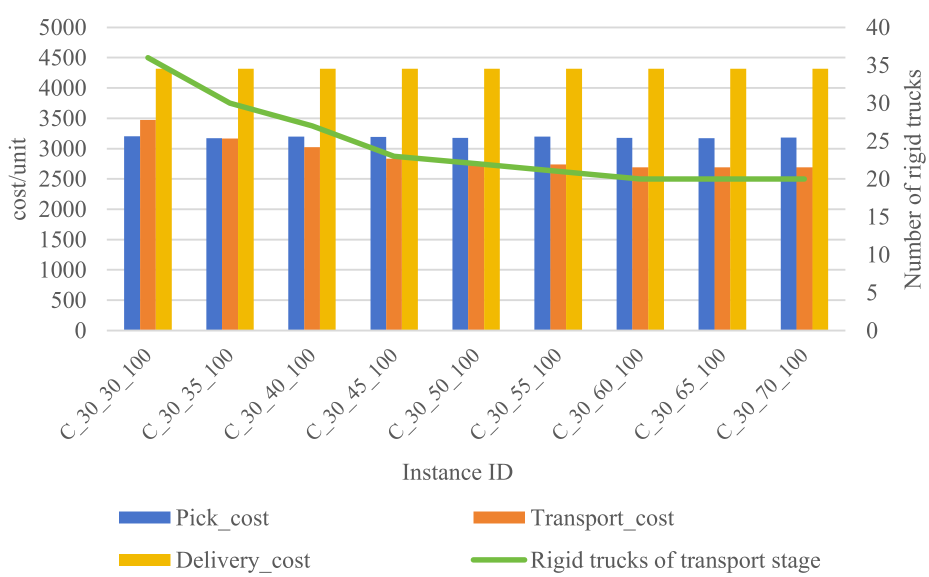

Fig. 14. Impact of rigid truck capacity.

analyzing the performance of multiple transport modes (Basic scenario and Scenario I) versus the single-transport mode (Scenario II, Scenario III, and Scenario IV), we found that a multimodal transport service, with relatively moderate costs and the ability to meet diverse customer preferences regarding time and cost, could be applied as a logistics service in urban logistics. In addition, we investigated the impact of store distributions and found that compared with the random distribution, the cost of the cluster distribution could save 13.02 % on average in the pickup stage. The same managerial insights have been discussed: concentration and specialization are the primary methods for improving efficiency and reducing costs in the logistics industry (Liu et al., 2022). Finally, a typical inverse relationship exists between vehicle capacity and the number of vehicles. An expected outcome confirmed by analyzing studies on rigid truck capacity is that logistics companies do not recommend blindly increasing vehicle capacity to reduce the number of vehicles and transport costs, especially when it reaches a critical threshold.

Future research may consider the following. Because a random utility discrete choice model is utilized to allocate commodities, and a demand–supply balance must be achieved, the number of commodities must be predetermined. Thus, one research direction is to extend the problem by considering commodities as uncertain and dynamic. In addition, the number of SE vehicles used in the SE is relatively large. Hence, another promising research direction is the 2E-VRP with multiple trips along the SE by SE vehicles for multiple SE routes.

CRediT authorship contribution statement

Shuai Wang: Conceptualization, Methodology, Software, Formal analysis, Investigation, Writing – original draft, Writing – review & editing, Visualization. **Xiaoning Zhu:** Resources, Conceptualization, Supervision, Funding acquisition. **Pan Shang:** Conceptualization, Data curation, Supervision, Writing – review & editing. **Xiao Lin:** Formal analysis, Investigation, Writing – review & editing. **Liya Yang:** Supervision, Writing – review & editing. **Lóránt Tavasszy:** Methodology, Validation, Formal analysis, Supervision, Writing – review & editing.

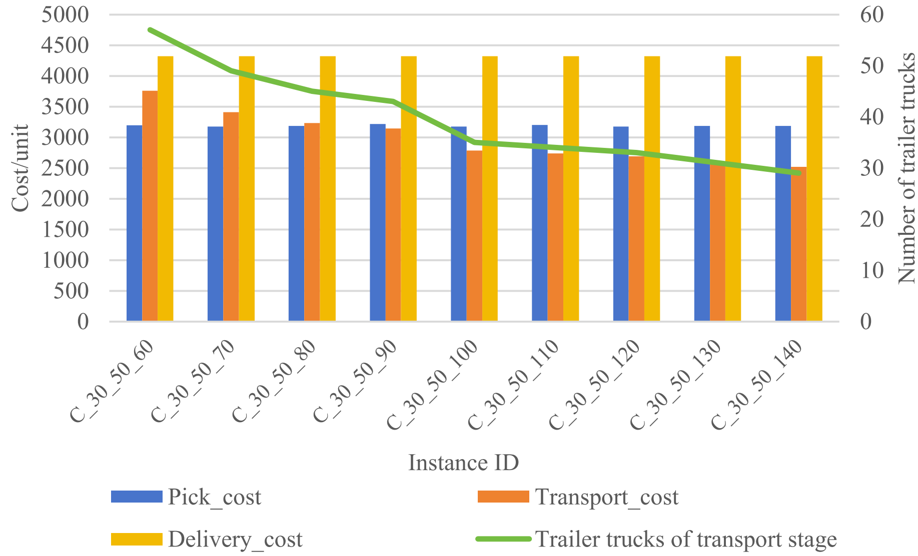

Fig. 15. Impact of trailer truck capacity.

Declaration of competing interest

The authors declare that they have no known competing financial interests or personal relationships that could have appeared to influence the work reported in this paper.

Data availability

I have shared the link to my date in our manuscript

Acknowledgments

This work has been supported by the Fundamental Research Funds for the Central Universities (No. 2023JBMC004), the Joint Funds of the National Natural Science Foundation of China (Nos. U2034208 and U2333218), the National Natural Science Foundation of China (Nos. 72001020, 72288101, 72074215), and Beijing Natural Science Foundation (No. 8242016).

Appendix A. Structures of destroy and repair operators

The structure of destroy operators is provided in **Algorithm 2**.

Algorithm 2 The structure of destroy operators
Input: The current solution s, the predetermined removal number l_r
Output: A partial solution s_p
Initialize removal list $L_r = \varnothing$, $r = 0$
While $r < l_r$, **do**
Applying a destroy operator to remove store node p
$L_r = L_r \cup p$
$r := r + 1$
Return removal list L_r and a partial solution s_p

The structure of repair operators is shown in **Algorithm 3**.

Algorithm 3 The structure of repair operators
Input: Partial solution s_p, the removal list L_r
Output: a new solution $s^{'}$
For store node of the removal list $p \in L_r$, **do**
Applying repair operator to insert store node p
If store node p cannot be inserted into any path, constructing a new path.
Return a new solution $s^{'}$

Appendix B. Parameters in the proposed ALNS algorithm

Table B1
Parameter values in ALNS.

Parameter	Value/Percentage gaps					
Initial temperature parameter δ	0.1					
Cooling rate c	0.94					
The adaptive weights parameter η	0.2					
The ratio of random removal	0.1–0.3					
The number of worst removals	4–14					
First Shaw parameter μ_1	0.5					
Second Shaw parameter μ_2	0.3					
Third Shaw parameter μ_3	0.2					
The ratio of Shaw removal	0.3					
The route removal number	1					
The route redistribution number	3					
Coefficient of regret-n	4					
Best new solution σ_1	>0.1	25	>0.01	16	<0.01	9
Improving solution σ_2		5		4		3
Deteriorating solution σ_3		1		1		1

Appendix C. Detailed computational results for the Beijing Yizhuang transportation network

Table C1
Computational results for the basic scenario.

Instance	S	D	Pickup stage		Transport stage					Delivery stage					
			C_1	C_2	C_3	C_4	C_5	C_6	C_7	C_8	C_9	C_{10}	C_{11}	C_{12}	C_{13}
B_1	282	2833	1036.09	1070	588.88	400	346.97	720	147.22	591.15	400	706.62	800	636.84	440
B_2	285	2809	1014.62	1050	588.88	400	333.84	690	147.22	578.78	400	719.38	800	617.26	440
B_3	288	3032	1046.44	1160	588.88	400	363.28	750	147.22	613.71	400	735.15	870	606.45	410
B_4	295	2996	1065.46	1150	588.88	400	373.24	780	147.22	568.08	380	750.12	870	633.83	450
B_5	316	3221	1201.60	1240	588.88	400	379.59	780	147.22	599.96	400	771.63	930	622.48	430
B_6	333	3388	1334.07	1280	588.88	400	389.55	810	147.22	621.79	410	784.48	980	605.86	450
B_7	333	3419	1301.54	1290	588.88	400	399.51	840	147.22	604.74	420	759.48	970	641.59	450
B_8	334	3315	1356.22	1240	588.88	400	402.69	840	147.22	579.04	420	763.86	940	631.53	450
B_9	346	3540	1304.04	1360	588.88	400	419.00	870	147.22	616.69	420	785.97	1030	636.32	470
B_10	363	3732	1445.59	1390	588.88	400	461.57	960	147.22	614.41	400	797.30	1070	616.23	470
B_11	389	3876	1476.78	1460	588.88	400	461.57	960	147.22	618.99	440	816.62	1160	628.59	500
B_12	395	4058	1526.01	1550	588.88	400	474.71	990	147.22	633.19	450	833.25	1120	637.45	470
B_13	396	4092	1536.80	1550	615.15	420	477.88	990	147.22	628.07	440	819.58	1190	627.34	490
B_14	403	4177	1572.48	1580	641.41	440	487.84	1020	147.22	642.06	450	853.22	1200	644.83	470
B_15	437	4428	1716.38	1660	615.15	420	553.08	1140	147.22	632.12	450	876.32	1270	613.94	470
B_16	475	4923	1891.00	1900	667.68	460	595.66	1230	147.22	634.32	460	941.60	1410	624.01	480
B_17	477	4933	1840.12	1890	615.15	420	615.15	1260	147.22	636.32	470	935.77	1430	607.49	520
B_18	479	4954	1874.90	1880	720.22	500	582.53	1200	147.22	641.59	500	929.94	1330	622.11	490
B_19	482	4997	1833.55	1910	720.22	500	579.35	1200	147.22	645.17	510	944.90	1350	624.39	500
B_20	515	5332	2136.25	2030	641.41	440	654.55	1350	147.22	659.88	500	987.15	1450	631.34	510
B_21	557	5693	2129.04	2150	799.02	560	680.81	1410	147.22	645.63	550	1042.71	1530	616.84	480
B_22	566	5891	2087.49	2210	857.91	600	693.95	1440	147.22	637.58	550	1127.16	1580	632.05	530
B_23	567	5737	2149.70	2150	805.37	560	693.95	1440	147.22	636.23	550	1033.00	1550	625.74	520
B_24	568	5826	2230.52	2180	746.48	520	713.44	1470	147.22	639.89	540	1103.47	1600	616.30	490

S: number of stores; D: number of commodities; C_1, C_2: travel and fixed costs of SE vehicles in the pickup stage, respectively. In transport stage, C_3, C_4: travel and fixed costs of rigid trucks, C_5, C_6: travel and fixed costs of trailer trucks, respectively, and C_7: travel cost of public vehicles. In the delivery stage, C_8, C_9: travel and fixed costs of SE vehicles for rigid commodities, respectively, C_{10}, C_{11}: travel and fixed costs of SE vehicles for trailer commodities, respectively, and C_{12}, C_{13}: travel and fixed costs of SE vehicles for public commodities, respectively.

Table C2
Detailed results for instance B_12.

P	S	Rigid commodities	Trailer commodities	Public commodities	Pickup Stage		Transport stage					Delivery stage					
					C_1	C_2	C_3	C_4	C_5	C_6	C_7	C_8	C_9	C_{10}	C_{11}	C_{12}	C_{13}
1	41	7;6;9;5;8;9;16	33;38;36;38;41;39;43	9;9;7;6;6;7;10	145.66	150	58.89	40	42.58	90	14.72	61.63	40	79.23	110	61.63	40
2	39	10;8;5;5;9;9;5	35;32;33;27;31;38;38	14;13;13;12;9;12;11	128.58	140	58.89	40	45.75	90	14.72	61.63	40	72.91	90	67.13	50
3	42	10;14;13;9;9;9;11	47;43;38;43;47;40;42	8;11;6;12;12;9;12	169.35	160	58.89	40	58.89	120	14.72	51.03	40	83.55	120	64.12	60
4	40	13;9;8;12;8;8;13	41;49;37;43;36;46;36	8;14;17;12;11;6;9	172.17	170	58.89	40	42.58	90	14.72	67.13	50	87.69	110	63.80	60
5	38	8;14;11;12;8;13;9	38;36;36;34;34;39;31	15;11;14;12;13;11;14	145.82	160	58.89	40	58.89	120	14.72	67.13	50	88.62	120	61.63	40
6	39	13;8;8;10;7;8;12	41;40;38;43;33;40;36	10;10;12;7;7;10;11	163.03	160	58.89	40	42.58	90	14.72	61.63	40	79.23	110	61.63	40
7	39	8;11;9;10;10;12;9	38;38;38;31;39;38;34	13;13;13;13;11;18;10	148.04	160	58.89	40	42.58	90	14.72	67.13	50	85.59	110	67.13	50
8	38	8;11;7;11;9;14;11	33;35;29;38;28;37;38	9;13;11;12;11;15;11	140.23	150	58.89	40	42.58	90	14.72	67.13	50	79.23	110	61.63	40
9	39	10;7;11;9;12;9;14	35;39;35;30;31;30;33	11;14;14;8;9;16;14	143.86	150	58.89	up40	42.58	90	14.72	61.63	40	73.28	100	67.13	50
10	40	11;8;10;8;8;15;13	44;39;45;42;37;46;44	4;6;10;8;4;6;3	169.28	150	58.89	40	55.71	120	14.72	67.13	50	103.92	140	61.63	40

P: Period; the other symbols are the same as those in Table C1.

Table C3
Computational results for Scenario I.

Instance	Pickup stage		Transport stage					Delivery stage	
	C_1	C_2	C_3	C_4	C_5	C_6	C_7	MB_C_1	MB_C_2
MB_1	1036.09	1070	588.88	400	346.97	720	147.22	886.19	1270
MB_2	1014.62	1050	588.88	400	333.84	690	147.22	862.72	1230
MB_3	1046.44	1160	588.88	400	363.28	750	147.22	952.27	1300
MB_4	1065.46	1150	588.88	400	373.24	780	147.22	916.09	1310
MB_5	1201.60	1240	588.88	400	379.59	780	147.22	1008.61	1350
MB_6	1334.07	1280	588.88	400	389.55	810	147.22	1002.04	1470
MB_7	1301.54	1290	588.88	400	399.51	840	147.22	1062.98	1440
MB_8	1356.22	1240	588.88	400	402.69	840	147.22	1018.45	1380
MB_9	1304.04	1360	588.88	400	419.00	870	147.22	1008.13	1470
MB_10	1445.59	1390	588.88	400	461.57	960	147.22	1116.43	1470
MB_11	1476.78	1460	588.88	400	461.57	960	147.22	1083.40	1530
MB_12	1526.01	1550	588.88	400	474.71	990	147.22	1150.51	1620
MB_13	1536.80	1550	615.15	420	477.88	990	147.22	1201.38	1650
MB_14	1572.48	1580	641.41	440	487.84	1020	147.22	1180.18	1700
MB_15	1716.38	1660	615.15	420	553.08	1140	147.22	1254.57	1710
MB_16	1891.00	1900	667.68	460	595.66	1230	147.22	1344.15	1940
MB_17	1840.12	1890	615.15	420	615.15	1260	147.22	1358.51	1950
MB_18	1874.90	1880	720.22	500	582.53	1200	147.22	1375.41	1880
MB_19	1833.55	1910	720.22	500	579.35	1200	147.22	1350.25	1940
MB_20	2136.25	2030	641.41	440	654.55	1350	147.22	1438.06	2050
MB_21	2129.04	2150	799.02	560	680.81	1410	147.22	1482.17	2170
MB_22	2087.49	2210	857.91	600	693.95	1440	147.22	1549.98	2240
MB_23	2149.70	2150	805.37	560	693.95	1440	147.22	1515.95	2190
MB_24	2230.52	2180	746.48	520	713.44	1470	147.22	1460.22	2210

MB_C_1, MB_C_2: travel and fixed costs of SE vehicles for all commodities, respectively. The other symbols are the same as those listed in Table 4.

Table C4
Computational results for Scenario II.

Instance	Pickup Stage		Transport Stage		Delivery Stage	
	C_1	C_2	C_3	C_4	SRB_C_1	SRB_C_2
SRB_1	1036.09	1070	1931.45	1340	886.19	1270
SRB_2	1014.62	1050	1911.53	1320	862.72	1230
SRB_3	1046.44	1160	2029.31	1400	952.27	1300
SRB_4	1065.46	1150	2003.04	1380	916.09	1310
SRB_5	1201.60	1240	2199.62	1520	1008.61	1350
SRB_6	1334.07	1280	2284.78	1580	1002.04	1470
SRB_7	1301.54	1290	2174.21	1520	1062.98	1440
SRB_8	1356.22	1240	2193.27	1520	1018.45	1380
SRB_9	1304.04	1360	2323.75	1600	1008.13	1470
SRB_10	1445.59	1390	2572.01	1760	1116.43	1470
SRB_11	1476.78	1460	2494.06	1720	1083.40	1530
SRB_12	1526.01	1550	2651.66	1840	1150.51	1620
SRB_13	1536.80	1550	2697.85	1880	1201.38	1650
SRB_14	1572.48	1580	2697.85	1880	1180.18	1700
SRB_15	1716.38	1660	2900.78	2020	1254.57	1710
SRB_16	1891.00	1900	3129.12	2160	1344.15	1940
SRB_17	1840.12	1890	3116.41	2160	1358.51	1950
SRB_18	1874.90	1880	3161.74	2180	1375.41	1880
SRB_19	1833.55	1910	3129.97	2180	1350.25	1940
SRB_20	2136.25	2030	3254.10	2260	1438.06	2050
SRB_21	2129.04	2150	3601.08	2500	1482.17	2170
SRB_22	2087.49	2210	3698.94	2560	1549.98	2240
SRB_23	2149.70	2150	3665.46	2520	1515.95	2190
SRB_24	2230.52	2180	3620.99	2520	1460.22	2210

SRB_C_1, SRB_C_2: travel and fixed costs of SE vehicles in the delivery stage, respectively. The other symbols are the same as those listed in Table 4.

Table C5
Computational results for Scenario III.

Instance	Pickup stage		Transport stage		Delivery stage	
	C_1	C_2	C_5	C_6	STB_C_1	STB_C_2
STB_1	1036.09	1070	536.77	1110	886.19	1270
STB_2	1014.62	1050	549.91	1140	862.72	1230
STB_3	1046.44	1160	582.53	1200	952.27	1300
STB_4	1065.46	1150	566.22	1170	916.09	1310
STB_5	1201.60	1240	621.93	1290	1008.61	1350

(continued on next page)

Table C5 (*continued*)

Instance	Pickup stage		Transport stage		Delivery stage	
	C_1	C_2	C_5	C_6	STB_C_1	STB_C_2
STB_6	1334.07	1280	651.37	1350	1002.04	1470
STB_7	1301.54	1290	628.71	1320	1062.98	1440
STB_8	1356.22	1240	638.24	1320	1018.45	1380
STB_9	1304.04	1360	654.55	1350	1008.13	1470
STB_10	1445.59	1390	703.48	1440	1116.43	1470
STB_11	1476.78	1460	683.99	1410	1083.40	1530
STB_12	1526.01	1550	749.66	1560	1150.51	1620
STB_13	1536.80	1550	762.79	1590	1201.38	1650
STB_14	1572.48	1580	749.66	1560	1180.18	1700
STB_15	1716.38	1660	792.24	1650	1254.57	1710
STB_16	1891.00	1900	854.30	1770	1344.15	1940
STB_17	1840.12	1890	854.30	1770	1358.51	1950
STB_18	1874.90	1880	870.61	1800	1375.41	1880
STB_19	1833.55	1910	847.95	1770	1350.25	1940
STB_20	2136.25	2030	893.70	1860	1438.06	2050
STB_21	2129.04	2150	965.72	2010	1482.17	2170
STB_22	2087.49	2210	982.03	2040	1549.98	2240
STB_23	2149.70	2150	975.25	2010	1515.95	2190
STB_24	2230.52	2180	995.17	2070	1460.22	2210

STB_C_1, STB_C_2: travel and fixed costs of SE vehicles in the delivery stage, respectively. The other symbols are the same as those listed in Table 4.

Table C6
Computational results for Scenario IV.

Instance	Pickup Stage		Transport Stage	Delivery Stage	
	C_1	C_2	C_7	SPB_C_1	SPB_C_2
SPB_1	1036.09	1070	561.45	886.19	1270
SPB_2	1014.62	1050	553.08	862.72	1230
SPB_3	1046.44	1160	628.28	952.27	1300
SPB_4	1065.46	1150	603.81	916.09	1310
SPB_5	1201.60	1240	635.06	1008.61	1350
SPB_6	1334.07	1280	697.12	1002.04	1470
SPB_7	1301.54	1290	653.17	1062.98	1440
SPB_8	1356.22	1240	666.09	1018.45	1380
SPB_9	1304.04	1360	688.97	1008.13	1470
SPB_10	1445.59	1390	715.02	1116.43	1470
SPB_11	1476.78	1460	730.17	1083.40	1530
SPB_12	1526.01	1550	767.77	1150.51	1620
SPB_13	1536.80	1550	761.20	1201.38	1650
SPB_14	1572.48	1580	821.68	1180.18	1700
SPB_15	1716.38	1660	826.66	1254.57	1710
SPB_16	1891.00	1900	923.15	1344.15	1940
SPB_17	1840.12	1890	939.46	1358.51	1950
SPB_18	1874.90	1880	924.73	1375.41	1880
SPB_19	1833.55	1910	934.69	1350.25	1940
SPB_20	2136.25	2030	944.44	1438.06	2050
SPB_21	2129.04	2150	1140.80	1482.17	2170
SPB_22	2087.49	2210	1101.40	1549.98	2240
SPB_23	2149.70	2150	1125.86	1515.95	2190
SPB_24	2230.52	2180	1087.10	1460.22	2210

SPB_C_1, SPB_C_2: travel and fixed costs of SE vehicles in the delivery stage, respectively. The other symbols are the same as those listed in Table 4.

Table C7
Computational results for different distribution.

Instance	S	D	Random distribution		Cluster distribution	
			Pickup cost	SE vehicles	Pickup cost	SE vehicles
R_C_1	292	3029	2365.38	115	1957.46	114
R_C_2	295	2946	2225.00	114	1937.37	111
R_C_3	297	2992	2252.09	115	1970.28	113
R_C_4	304	3095	2333.55	120	1971.52	117
R_C_5	328	3332	2567.89	125	2179.24	126
R_C_6	335	3297	2521.47	123	2193.77	125
R_C_7	344	3566	2751.49	136	2366.72	132
R_C_8	345	3580	2708.53	137	2306.55	136
R_C_9	394	3973	3101.45	153	2616.62	149
R_C_10	397	4005	3084.84	152	2583.34	151
R_C_11	398	4090	3131.18	156	2711.94	159
R_C_12	399	4064	3108.63	152	2674.81	153

(*continued on next page*)

Table C7 (*continued*)

Instance	S	D	Random distribution		Cluster distribution	
			Pickup cost	SE vehicles	Pickup cost	SE vehicles
R_C_13	474	4856	3673.76	182	3234.73	182
R_C_14	477	4969	3676.89	186	3307.61	185
R_C_15	478	4925	3684.18	185	3399.24	186
R_C_16	479	4979	3876.51	190	3263.44	186
R_C_17	555	5735	4325.57	215	3870.63	210
R_C_18	557	5662	4223.84	212	3857.71	212
R_C_19	558	5657	4207.89	211	3787.00	209
R_C_20	563	5873	4426.49	220	3926.10	218

S: number of stores; *D*: number of commodities.

Table C8
Computational results for different vehicle capacities.

Instance	S	D	Pickup Stage		Transport Stage					Delivery Stage					
			C_1	C_2	C_3	C_4	C_5	C_6	C_7	C_8	C_9	C_{10}	C_{11}	C_{12}	C_{13}
C_20_50_100	408	4273	1704.11	2670	641.41	440	507.33	1050	147.22	673.82	590	1148.25	1640	624.90	590
C_25_50_100	408	4273	1630.93	1930	641.41	440	507.33	1050	147.22	638.97	520	939.47	1400	617.82	550
C_30_50_100	408	4273	1566.23	1610	641.41	440	507.33	1050	147.22	643.38	470	840.04	1220	626.05	520
C_35_50_100	408	4273	1509.61	1360	641.41	440	507.33	1050	147.22	627.29	420	810.06	1130	608.10	410
C_40_50_100	408	4273	1445.85	1230	641.41	440	507.33	1050	147.22	621.79	410	765.12	1000	608.10	410
C_45_50_100	408	4273	1422.41	1070	641.41	440	507.33	1050	147.22	616.30	400	740.91	880	602.60	400
C_50_50_100	408	4273	1415.38	980	641.41	440	507.33	1050	147.22	616.30	400	712.82	800	602.60	400
C_30_30_100	408	4273	1584.32	1620	1047.28	720	507.33	1050	147.22	643.38	470	840.04	1220	626.05	520
C_30_35_100	408	4273	1550.35	1620	864.26	600	507.33	1050	147.22	643.38	470	840.04	1220	626.05	520
C_30_40_100	408	4273	1578.21	1620	779.10	540	507.33	1050	147.22	643.38	470	840.04	1220	626.05	520
C_30_45_100	408	4273	1581.89	1610	667.68	460	507.33	1050	147.22	643.38	470	840.04	1220	626.05	520
C_30_50_100	408	4273	1566.23	1610	641.41	440	507.33	1050	147.22	643.38	470	840.04	1220	626.05	520
C_30_55_100	408	4273	1566.75	1630	615.15	420	507.33	1050	147.22	643.38	470	840.04	1220	626.05	520
C_30_60_100	408	4273	1565.72	1610	588.88	400	507.33	1050	147.22	643.38	470	840.04	1220	626.05	520
C_30_65_100	408	4273	1560.70	1610	588.88	400	507.33	1050	147.22	643.38	470	840.04	1220	626.05	520
C_30_70_100	408	4273	1562.97	1620	588.88	400	507.33	1050	147.22	643.38	470	840.04	1220	626.05	520
C_30_50_60	408	4273	1575.55	1620	641.41	440	821.68	1710	147.22	643.38	470	840.04	1220	626.05	520
C_30_50_70	408	4273	1547.24	1630	641.41	440	713.44	1470	147.22	643.38	470	840.04	1220	626.05	520
C_30_50_80	408	4273	1556.25	1630	641.41	440	654.55	1350	147.22	643.38	470	840.04	1220	626.05	520
C_30_50_90	408	4273	1597.17	1620	641.41	440	625.10	1290	147.22	643.38	470	840.04	1220	626.05	520
C_30_50_100	408	4273	1566.23	1610	641.41	440	507.33	1050	147.22	643.38	470	840.04	1220	626.05	520
C_30_50_110	408	4273	1569.07	1630	641.41	440	491.02	1020	147.22	643.38	470	840.04	1220	626.05	520
C_30_50_120	408	4273	1556.14	1620	641.41	440	474.71	990	147.22	643.38	470	840.04	1220	626.05	520
C_30_50_130	408	4273	1566.11	1620	641.41	440	445.26	930	147.22	643.38	470	840.04	1220	626.05	520
C_30_50_140	408	4273	1567.66	1620	641.41	440	419.00	870	147.22	643.38	470	840.04	1220	626.05	520

The symbols are the same as those in Table C1.

References

Anderluh, A., Hemmelmayr, V. C., & Nolz, P. C. (2017). Synchronizing vans and cargo bikes in a city distribution network. *Central European Journal of Operations Research, 25*, 345–376.

Baldacci, R., Mingozzi, A., Roberti, R., & Calvo, R. W. (2013). An exact algorithm for the two-echelon capacitated vehicle routing problem. *Operations Research, 61*(2), 298–314.

Bayliss, C., Bektaş, T., Tjon-Soei-Len, V., & Rohner, R. (2023). Designing a multi-modal and variable-echelon delivery system for last-mile logistics. *European Journal of Operational Research, 307*(2), 645–662.

Belgin, O., Karaoglan, I., & Altiparmak, F. (2018). Two-echelon vehicle routing problem with simultaneous pickup and delivery: Mathematical model and heuristic approach. *Computers & Industrial Engineering, 115*, 1–16.

Boccia, M., Crainic, T. G., Sforza, A., & Sterle, C. (2018). Multi-commodity location-routing: Flow intercepting formulation and branch-and-cut algorithm. *Computers & Operations Research, 89*, 94–112.

Breunig, U., Schmid, V., Hartl, R. F., & Vidal, T. (2016). A large neighbourhood based heuristic for two-echelon routing problems. *Computers & Operations Research, 76*, 208–225.

Cebeci, M. S., Tapia, R. J., Kroesen, M., de Bok, M., & Tavasszy, L. (2023). The effect of trust on the choice for crowdshipping services. *Transportation Research Part A: Policy and Practice, 170*, Article 103622.

Crainic, T. G., Ricciardi, N., & Storchi, G. (2009). Models for evaluating and planning city logistics systems. *Transportation science, 43*(4), 432–454.

Crainic, T. G., Errico, F., Rei, W., & Ricciardi, N. (2016). Modeling demand uncertainty in two-tier city logistics tactical planning. *Transportation Science, 50*(2), 559–578.

Cuda, R., Guastaroba, G., & Speranza, M. G. (2015). A survey on two-echelon routing problems. *Computers & Operations Research, 55*, 185–199.

Dellaert, N., Van Woensel, T., Crainic, T. G., & Saridarq, F. D. (2021). A multi-commodity two-echelon capacitated vehicle routing problem with time windows: Model formulations and solution approach. *Computers & Operations Research, 127*, Article 105154.

Fontaine, P., Crainic, T. G., Jabali, O., & Rei, W. (2021). Scheduled service network design with resource management for two-tier multimodal city logistics. *European Journal of Operational Research, 294*(2), 558–570.

Grangier, P., Gendreau, M., Lehuédé, F., & Rousseau, L. M. (2016). An adaptive large neighborhood search for the two-echelon multiple-trip vehicle routing problem with satellite synchronization. *European Journal of Operational Research, 254*(1), 80–91.

Gu, W., Archetti, C., Cattaruzza, D., Ogier, M., Semet, F., & Speranza, M. G. (2022). A sequential approach for a multi-commodity two-echelon distribution problem. *Computers & Industrial Engineering, 163*, Article 107793.

Hemmelmayr, V. C., Cordeau, J. F., & Crainic, T. G. (2012). An adaptive large neighborhood search heuristic for two-echelon vehicle routing problems arising in city logistics. *Computers & Operations Research, 39*(12), 3215–3228.

Jia, S., Deng, L., Zhao, Q., & Chen, Y. (2023). An adaptive large neighborhood search heuristic for multi-commodity two-echelon vehicle routing problem with satellite synchronization. *Journal of Industrial and Management Optimization, 19*(2), 1187–1210.

Jie, W., Yang, J., Zhang, M., & Huang, Y. (2019). The two-echelon capacitated electric vehicle routing problem with battery swapping stations: Formulation and efficient methodology. *European Journal of Operational Research, 272*(3), 879–904.

Kancharla, S. R., & Ramadurai, G. (2019). Multi-depot two-echelon fuel minimizing routing problem with heterogeneous fleets: Model and heuristic. *Networks and Spatial Economics, 19*, 969–1005.

Khakdaman, M., Rezaei, J., & Tavasszy, L. A. (2020). Shippers' willingness to delegate modal control in freight transportation. *Transportation Research Part E: Logistics and Transportation Review, 141*, Article 102027.

Kim, B., Jeong, H. Y., & Lee, S. (2023). Two-echelon collaborative routing problem with heterogeneous crowd-shippers. *Computers & Operations Research, 160*, Article 106389.

Liu, S., He, N., Cao, X., Li, G., & Jian, M. (2022). Logistics cluster and its future development: A comprehensive research review. *Transportation Research Part E: Logistics and Transportation Review, 168*, Article 102974.

Liu, Y., Lyu, C., Liu, Z., & Cao, J. (2021). Exploring a large-scale multi-modal transportation recommendation system. *Transportation Research Part C: Emerging Technologies, 126*, Article 103070.

Marques, G., Sadykov, R., Deschamps, J. C., & Dupas, R. (2020). An improved branch-cut-and-price algorithm for the two-echelon capacitated vehicle routing problem. *Computers & Operations Research, 114*, Article 104833.

Najmi, A., Rashidi, T. H., & Waller, T. (2023). A multimodal multi-provider market equilibrium model: A game-theoretic approach. *Transportation Research Part C: Emerging Technologies, 146*, Article 103959.

Perboli, G., Tadei, R., & Vigo, D. (2011). The two-echelon capacitated vehicle routing problem: Models and math-based heuristics. *Transportation Science, 45*(3), 364–380.

Perboli, G., Rosano, M., Saint-Guillain, M., & Rizzo, P. (2018). Simulation–optimisation framework for City Logistics: An application on multimodal last-mile delivery. *IET Intelligent Transport Systems, 12*(4), 262–269.

Ropke, S., & Pisinger, D. (2006). An adaptive large neighborhood search heuristic for the pickup and delivery problem with time windows. *Transportation Science, 40*(4), 455–472.

Ropke, S., & Pisinger, D. (2006). A unified heuristic for a large class of vehicle routing problems with backhauls. *European Journal of Operational Research, 171*(3), 750–775.

Santos, F. A., Mateus, G. R., & da Cunha, A. S. (2015). A branch-and-cut-and-price algorithm for the two-echelon capacitated vehicle routing problem. *Transportation Science, 49*(2), 355–368.

Shaw, P. (1998, October). Using constraint programming and local search methods to solve vehicle routing problems. *In International conference on principles and practice of constraint programming* (pp. 417-431). Berlin, Heidelberg: Springer Berlin Heidelberg.

Sluijk, N., Florio, A. M., Kinable, J., Dellaert, N., & Van Woensel, T. (2023). Two-echelon vehicle routing problems: A literature review. *European Journal of Operational Research, 304*(3), 865–886.

Tapia, R. J., Kourounioti, I., Thoen, S., de Bok, M., & Tavasszy, L. (2023). A disaggregate model of passenger-freight matching in crowdshipping services. *Transportation Research Part A: Policy and Practice, 169*, Article 103587.

Train, K. E. (2009). *Discrete choice methods with simulation*. Cambridge University Press.

Vincent, F. Y., Jodiawan, P., Schrotenboer, A. H., & Hou, M. L. (2023). The two-echelon vehicle routing problem with time windows, intermediate facilities, and occasional drivers. *Expert Systems with Applications, 234*, Article 120945.

Wang, K., Lan, S., & Zhao, Y. (2017). A genetic-algorithm-based approach to the two-echelon capacitated vehicle routing problem with stochastic demands in logistics service. *Journal of the Operational Research Society, 68*(11), 1409–1421.

Wicaksono, S., Lin, X., & Tavasszy, L. A. (2022). Market potential of bicycle crowdshipping: A two-sided acceptance analysis. *Research in Transportation Business & Management, 45*, Article 100660.

Yıldız, E. A., Karaoğlan, İ., & Altiparmak, F. (2023). An exact algorithm for two-echelon location-routing problem with simultaneous pickup and delivery. *Expert Systems with Applications*, Article 120598.

Zhou, H., Qin, H., Cheng, C., & Rousseau, L. M. (2023). An exact algorithm for the two-echelon vehicle routing problem with drones. *Transportation Research Part B: Methodological, 168*, 124–150.

Zhou, L., Baldacci, R., Vigo, D., & Wang, X. (2018). A multi-depot two-echelon vehicle routing problem with delivery options arising in the last mile distribution. *European Journal of Operational Research, 265*(2), 765–778.

Zhou, S., Zhang, D., Ji, B., & Li, S. (2024). Two-echelon vehicle routing problem with direct deliveries and access time windows. *Expert Systems with Applications, 244*, Article 121150.